

OXYGEN ABSORPTION ENHANCED BY SULFITE OXIDATION CATALYZED WITH
MANGANESE AND IRON

BY

ROBERTO EDUARDO PRADA

THESIS

Presented to the Faculty of the Graduate School of
The University of Texas at Austin
in Partial Fulfillment
of the Requirements
for the Degree of

MASTER OF SCIENCE IN ENGINEERING

THE UNIVERSITY OF TEXAS AT AUSTIN

December, 1981

ABSTRACT

Oxygen absorption across an unbroken gas/liquid interface enhanced by sulfite oxidation catalyzed with manganese and iron and inhibited by sulfate has been studied. Using approximate solutions to the penetration theory a model was developed for the manganese catalyzed oxidation at pH 5 and 0.01 M total sulfite. The model predicts first order kinetics in manganese. The kinetics are first order in oxygen at low oxygen pressures, and zero order at high oxygen pressures. A significant increase of O_2 absorption was observed for manganese concentrations greater than 1 mM. The presence of iron greatly increases the O_2 absorption rate at manganese concentrations greater than 1 mM. At an iron concentration of 0.3 to 3 mM and pH 4, there is a threshold manganese concentration of 1 to 2 mM above which there is a discontinuous enhancement of 20 to 100 from physical absorption, and an enhancement of 10 from the absorption with no iron present. It is recommended that further work be done to quantify simultaneous SO_2 and O_2 with catalysis by Mn/Fe. Thiosulfate proved to be a powerful inhibitor of the sulfite oxidation reaction. A 1 mM thiosulfate concentration reduces the reaction rate by a factor of about 400.

TABLE OF CONTENTS

	Page
ABSTRACT	v
TABLE OF CONTENTS	vi
LIST OF FIGURES	viii
LIST OF TABLES	ix
CHAPTER I: INTRODUCTION	1
Process Technology	1
Literature Review	3
CHAPTER II: THEORY	8
CHAPTER III: EXPERIMENTAL APPARATUS AND PROCEDURE	11
Methodology	11
Apparatus	12
Procedure	16
Data Analysis	18
CHAPTER IV: RESULTS AND DISCUSSION	20
Manganese	20
Manganese and Iron	28
Thiosulfate	34
CHAPTER V: CONCLUSIONS AND RECOMMENDATIONS	36
Conclusions	36
Recommendations	37

	Page
APPENDIX A: EXPERIMENTAL DATA	38
APPENDIX B: SULFITE, pH, IONIC STRENGTH AND ELECTROLYTE DATA .	44
APPENDIX C: GAS FLOW SYSTEM	53
APPENDIX D: MASS BALANCE AT THE INTERFACE	57
APPENDIX E: NOTATION	63
REFERENCES CITED	66
VITA	70

LIST OF FIGURES

Figure		Page
1.1	Throwaway Slurry Scrubbing	2
1.2	Forced Oxidation in the Throwaway Scrubbing Loop . . .	4
3.1	Experimental Apparatus	13
3.2	Detailed Components of Reactor	14
3.3	Top View of Reactor Showing Orientations of Each Component	15
4.1	Comparison of Calculated and Measured Values of the Enhancement Factor	23
4.2	Enhancement Factor as a Function of Manganese Concentration	25
4.3	Mass Transfer Coefficient as a Function of O_2 Partial Pressure and Manganese Concentration	26
4.4	Mass Transfer Coefficient as a Function of Manganese Concentration and Temperature	29
4.5	Mass Transfer Coefficient as a Function of Iron Concentration and O_2 Partial Pressure	31
4.6	Enhancement Factor as a Function of Mn and Fe	32
4.7	Inhibiting Effect of Thiosulfate	35
C.1	Oxygen Rotameter Calibration Curve	55
C.2	Nitrogen Rotameter Calibration Curve	56

LIST OF TABLES

Table		Page
4.1	Experimental Constants	21
A.1	Experimental Data - Mn Catalyzed Oxidation	39
A.2	Experimental Data - Mn/Fe Catalyzed Oxidation	41
A.3	Experimental Data - Thiosulfate Inhibited Oxidation.	43
B.1	Experimental Data - Dependence on Sulfite Conc.	46
B.2	Experimental Data - pH Dependence	49
B.3	Experimental Data - Dependence on Na_2SO_4 Conc.	51
B.4	Experimental Data - Dependence on Electrolyte	52
D.1	Constants for the Mass Balance at the Interface	60
D.2	Comparison of Bulk and Interface pH and Total Sulfite Concentration at 50°C	61

CHAPTER I

INTRODUCTION

This work is a study of the enhancement of oxygen absorption into aqueous solutions by sulfite oxidation catalyzed with manganese and iron. Some experimental data with thiosulfate, a known inhibitor of the reaction, are also presented. The experimental conditions were chosen to relate closely to the operating conditions in throwaway scrubbing systems: 50°C, pH 4-5, oxygen partial pressures of 0.018 to 0.878 atm, catalyst concentrations of 10^{-6} to 10^{-1} M, and total sulfite ($\text{SO}_3^{-2} + \text{HSO}_3^{-}$) concentration of 10^{-2} M. The results and conclusions of this work are applicable to natural oxidation in the scrubber, and to forced oxidation in the scrubber loop or in a bleed stream.

Process Technology

Throwaway scrubbing (Figure 1.1) is the most widely used process to control SO_2 emissions into the atmosphere. The process uses either slurry scrubbing or clear solution scrubbing. The SO_2 waste gas is absorbed into the aqueous solution at a pH of 5 to 6. Because 5 to 10% of the flue gas is O_2 , 10 to 100% of the absorbed SO_2 is naturally oxidized to sulfate. Limestone and/or lime is added to the crystallizer as a source of Ca^{+2} and alkalinity. The solution is then recycled to the scrubber and a fraction containing 10 to 15% solids is withdrawn to a solid-liquid separator where $\text{CaSO}_3/\text{CaSO}_4$ solids are collected and the liquid portion is returned to the scrub-

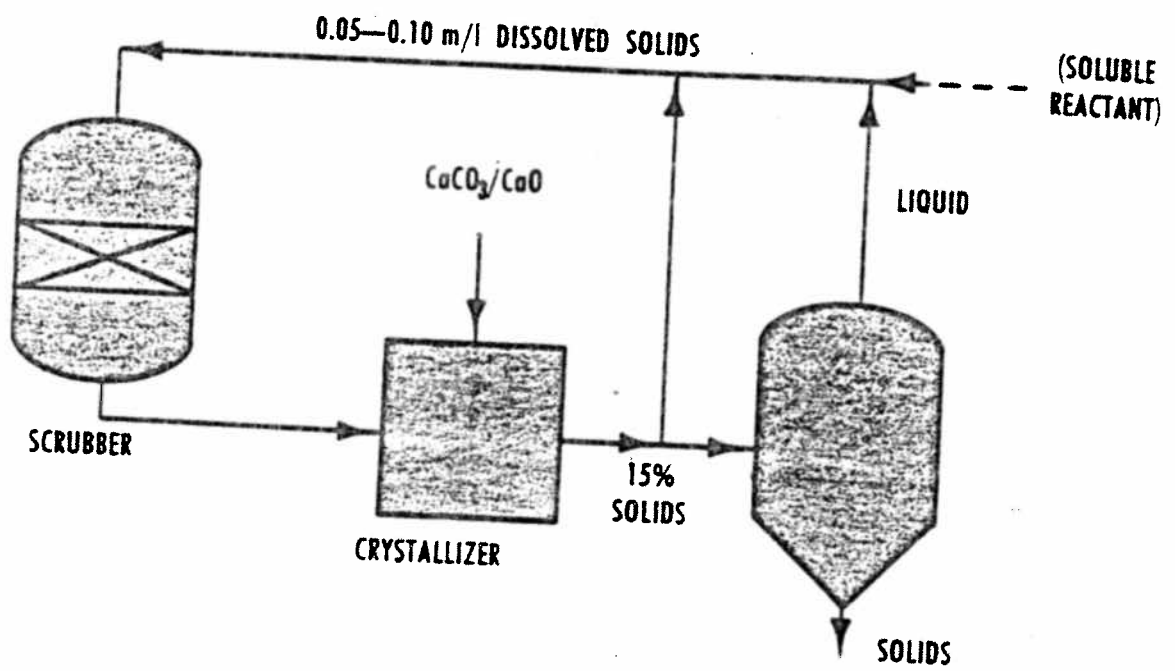


Figure 1.1: Throwaway Slurry Scrubbing

ber. The $\text{CaSO}_3/\text{CaSO}_4$ solids are disposed of in ponds or in landfills.

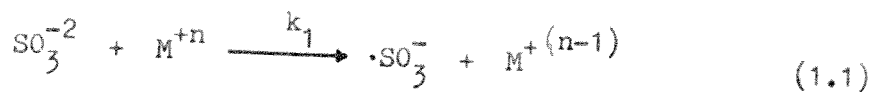
There are several alternatives to throwaway scrubbing which are presented by Rochelle and King (1978). One such an alternative, used mainly in Japan, includes intentional oxidation in the scrubber loop (Figure 1.2), where the oxygen source is air, and the final solid product is gypsum. In Japan, the gypsum ($\text{CaSO}_4 \cdot 2\text{H}_2\text{O}$) has been sold for use in wallboard. It is also more easily dewatered than CaSO_3 waste solids and is more suitable for landfill disposal.

Literature Review

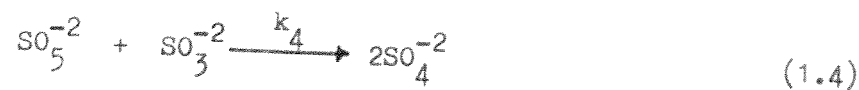
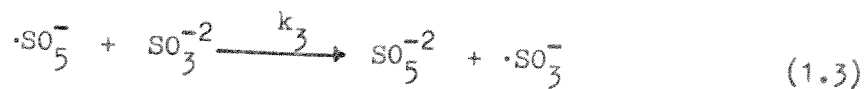
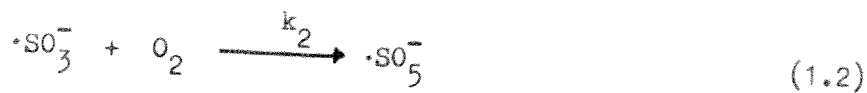
Previous study of sulfite oxidation kinetics has been carried out in two different types of experiments: homogeneous, in which the reaction occurs in the bulk of the solution; and heterogeneous, in which oxygen is absorbed into a sulfite solution.

The sulfite oxidation free radical chain mechanism presented below was originally proposed by Backstrom (1934). This mechanism with some slight modifications (Brimblecombe and Spedding, 1974a; Hayon et al, 1972) is generally accepted.

Initiation:



Propagation:



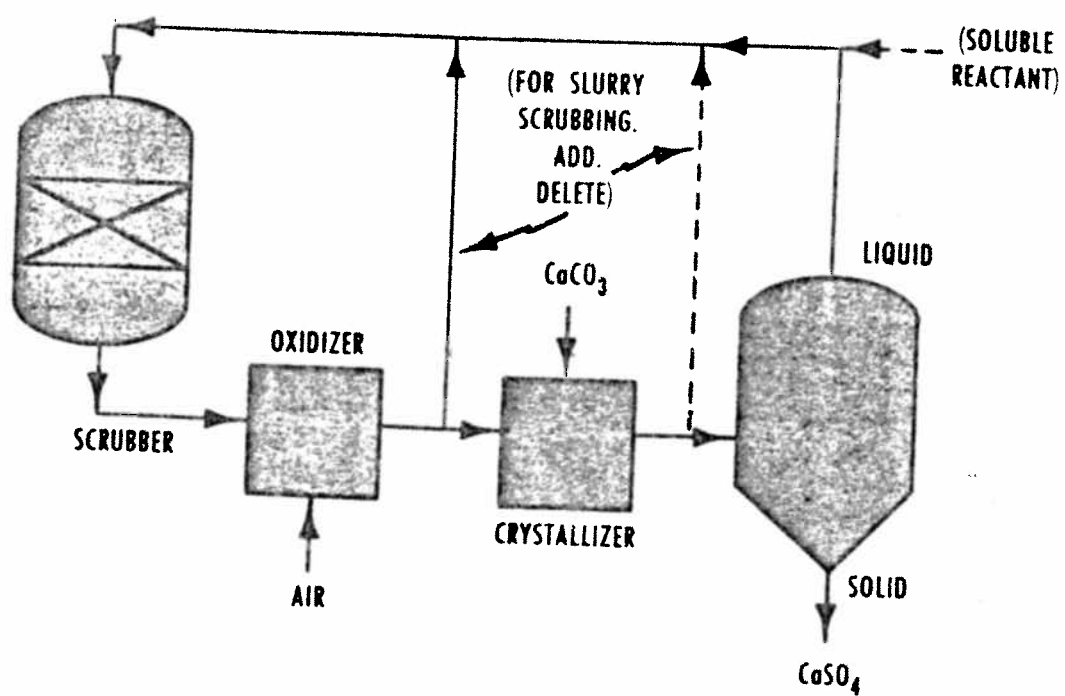
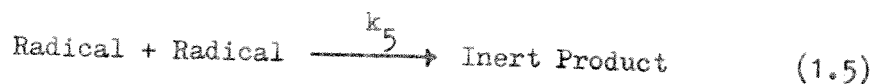


Figure 1.2: Forced Oxidation in the Throwaway Scrubbing Loop

Termination:



where M^{+n} is the catalyst at oxidation state $+n$ (Co^{+3} , Cu^{+2} , Mn^{+3} , Fe^{+3}).

Assuming that reaction 1.2 is fast and that reaction 1.5 is primarily a combination of two $\cdot\text{SO}_5^-$ radicals, and using the steady state assumption for the radical ions, the following rate expression is derived:

$$r = K [M^{+n}]^{1/2} [\text{SO}_3^{2-}]^{3/2} [\text{O}_2]^0 \quad (1.6)$$

where $K = k_3(k_1/k_5)^{1/2}$

Most of the experimentation done so far in the kinetics of sulfite oxidation has been done with cobalt or copper as catalyst. It is generally accepted that under homogeneous conditions equation 1.6 represents the reaction kinetics catalyzed by cobalt (Mishra and Srivastava, 1976; Chen and Barron, 1972; Bengtsson and Bjerle, 1975) and by copper (Barron and O'Hern, 1966; Mishra and Srivastava, 1976). However there is some disagreement under heterogeneous conditions. Several researchers found the kinetics to be zero order in sulfite, second order in oxygen, and first order in cobalt (Reith and Beek, 1973; Wesselingh and van't Hoog, 1970; Sawicki and Barron, 1974; Laurent et al, 1974). Others found the oxygen order to be 2

at low oxygen partial pressures and 1 at higher oxygen partial pressures (Linek and Mayhoferova, 1970; Alper, 1973; Nyvlt and Kastanek, 1975; Onda et al, 1971). Astarita et al (1964) found sulfite to inhibit the reaction at high concentrations. An excellent review of the state-of-the-art under homogeneous and heterogeneous conditions with cobalt and copper has been published by Linek and Vacek (1981).

A lesser amount of information is available for the catalyzed reaction with manganese and iron. Most of the conclusions have been qualitative and no general mechanism or rate expression is available as yet. Brimblecombe and Spedding (1974a) found the iron order in the reaction to be 1 at a pH of 3.8 and to steadily increase with pH to an order of 1.8 at pH 5. For the manganese catalyzed reaction they proposed a two-rate expression in which the manganese order is one; the term which dominates at low pH values is first order in sulfite and the one that dominates at high pH values is second order in sulfite. Using a homogeneous system at 25°C, Coughanowr and Krause (1965) found the manganese, sulfur dioxide, and oxygen orders to be two, zero, and zero, respectively. Braga and Connick (1981) found the reaction rate to be independent of the sulfite and oxygen concentrations, the manganese order to be $3/2$, and the hydrogen ion order to be -1 in the pH range of 3 to 4.7. In acidified solutions, Bassett and Parker (1951) found manganese to be a more effective catalyst than Co, Fe, and Cu. They contend that this phenomenon is due to the

greater capability of manganese to form sulfite complexes, and that cobalt acts similarly to manganese, yet not as effective nor as selective towards sulfate. Johnstone and Coughanowr (1958) observed that 250 ppm of MnSO_4 were as effective as 50,000 ppm of $\text{Fe}_2(\text{SO}_4)_3$ in the absorption and oxidation of SO_2 by drops of catalyst solutions.

Hudson (1980) experimented with manganese and iron combined. He noted that the reaction is zero order with respect to iron, but the overall rates were significantly greater than those with no iron present. He also concluded that the rate does not depend on the amount of iron for $\text{Fe} > 1$ ppm.

Chertkov (1959) contended that thiosulfate is a catalyst of the sulfite oxidation reaction. Linek and Mayhoferova (1970) found no effect of thiosulfate up to a concentration of 10^{-5} M. However, more recent data obtained by Hudson (1979) and Radian (1977) suggest that thiosulfate is a powerful inhibitor of the reaction.

CHAPTER II

THEORY

Mass transfer with simultaneous chemical reaction involves such complicated mathematical analysis that an analytical solution is rarely obtained. In this chapter an effort is made to simplify the equations and solutions of the mathematical treatment involved in the particular problem of oxygen absorption into a sulfite solution in an agitated batch reactor.

The penetration model dictates the following expressions:

$$D_o \frac{\partial^2 [O_2]}{\partial x^2} = \frac{\partial [O_2]}{\partial t} + r_o \quad (2.1)$$

and,

$$D_s \frac{\partial^2 [SO_3^{-2}]}{\partial x^2} = \frac{\partial [SO_3^{-2}]}{\partial t} + r_s \quad (2.2)$$

where x is the distance from the surface, D_o and D_s are the diffusivities of oxygen and sulfite, respectively, r_o is the rate of oxygen disappearance by reaction, and r_s is the sulfite reaction rate, which is equal to $2r_o$.

In the work presented here the sulfite concentration was maintained at high levels (0.01 M) so that its reaction with oxygen could not be limited by sulfite diffusion from the bulk to the surface. Therefore, equation 2.2 may be dropped from any further treatment.

The initial condition for equation 2.1 is:

$$[O_2] = 0 \quad \text{at } t = 0, x > 0 \quad (2.1a)$$

and the boundary conditions are:

$$[O_2] = [O_2]^* \quad \text{at } t > 0, x = 0 \quad (2.1b)$$

$$[O_2] = 0 \quad \text{at } t > 0, x = \infty \quad (2.1c)$$

where $[O_2]^*$ is the equilibrium oxygen concentration in the aqueous solution at a particular temperature and oxygen partial pressure.

Equation 2.1 has an analytical solution only for the case where the rate of reaction is first order in oxygen; that is, $r_o = k' [O_2]$, (Danckwerts, 1970):

$$\bar{R} = k_L^o [O_2]^* \left(1 + \frac{D_o k'}{(k_L^o)^2} \right)^{1/2} \quad (2.3)$$

The enhancement factor, E is defined as:

$$E = \frac{\bar{R}}{k_L^o [O_2]^*} = \frac{k_L}{k_L^o} = \left(1 + \frac{D_o k'}{(k_L^o)^2} \right)^{1/2} \quad (2.4)$$

Since the oxidation rate may not be first order in oxygen, it is desired to obtain an absorption rate expression for the more general case of mth order in oxygen ($r_o = k' [O_2]^m$). Hikita and Asai (1964) linearized the kinetic rate equation by the assumption:

$$r_o = k' [O_2]^{*(m-1)} [O_2] \quad (2.5)$$

Using the film model they compared the solution obtained by applying their assumption to the actual solution obtained by numerical methods.

In their nomenclature the kinetic factor, γ is defined by:

$$\gamma = \left(\frac{2 k' [O_2]^{*(m-1)} D_o}{(m+1) (k_L^\circ)^2} \right)^{1/2} \quad (2.6)$$

They found that the ratio of the enhancement factor with no assumption to that obtained making a use of their assumption (Equation 2.5) to have a maximum difference from 1 at a γ value of 1.3 for all values of m . At this γ value the enhancement factor ratios are 1.09 and 0.94 for m equal to infinity and equal to zero, respectively. The ratios for all other positive m values fall in between these two values, the ratio being 1.0 for m equal to one. For γ values less than 0.1 and greater than 10 the enhancement factor ratios are essentially 1.0 for all values of m .

Since the Hikita assumption (Equation 2.5) has proven to be an excellent one, equation 2.1 is now solved making use of it:

$$\bar{R} = k_L^\circ [O_2]^* \left(1 + \frac{D_o k' [O_2]^{*(m-1)}}{(k_L^\circ)^2} \right)^{1/2} \quad (2.7)$$

where k' is a function of catalyst and sulfite concentrations, pH, and temperature.

CHAPTER III

EXPERIMENTAL APPARATUS AND PROCEDURE

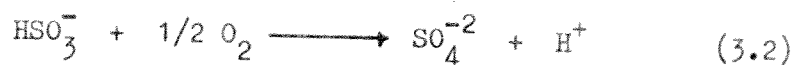
Oxygen was absorbed from nitrogen gas across an unbroken gas/liquid interphase into an agitated sulfite/bisulfite solution. Constant pH and total dissolved sulfite were maintained by titrating with sodium sulfite solution. The O_2 absorption rate was determined directly from the quantity of titrant added. $MnSO_4$, $FeSO_4$, and $Na_2S_2O_3$ were added in varying amounts to catalyze or inhibit the oxidation.

Methodology

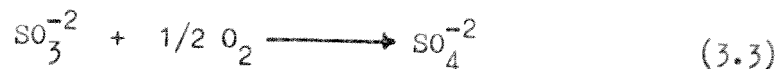
The experiments were performed in sulfite/bisulfite solutions buffered by the equilibrium:



Because bisulfite oxidation would create a H^+ by the stoichiometry,



the pH of the solution was controlled at a constant value by titration with Na_2SO_3 solution. The net stoichiometry of the oxidation reaction at constant pH is given by:



Note that sulfite is added to the solution at the same rate that it is consumed to form sulfate, and that no net production or

consumption of H^+ occurs. Hence, all the concentrations in the reactor solution are kept constant except for that of sulfate. Furthermore, the rate of oxygen absorption will be one half the sulfite titration rate.

Apparatus

The apparatus is shown in Figure 3.1. It consisted of a three liter plexiglass batch reactor, an automatic burette/dispenser, an electrometer, and a titrate demand module. Oxygen and nitrogen were supplied by two large cylinders.

The reactor was 14 cm in diameter with an O-ring sealed lid. It was baffled on four sides to eliminate vortex effects. The detailed components of the reactor are shown in Figure 3.2. A variable speed agitator with a three bladed 2.5 cm marine propeller was used. The agitation speed was measured by counting the revolutions per minute of a reduced gear shaft turning at 1/12 the speed of the main shaft. The agitation speed was kept constant at 470 rpm for all runs. At 470 rpm there were no gas bubbles in the solution and the gas/liquid contact area could be estimated assuming a planar surface. Figure 3.3 shows the orientation of the various components in the reactor. All devices were fastened to the reactor lid by means of number three and four rubber stoppers.

The oxygen/nitrogen mixture was introduced to the reactor through a fritted glass dispersion tube above the liquid surface. The flow rate of each gas was measured by a rotameter and controlled

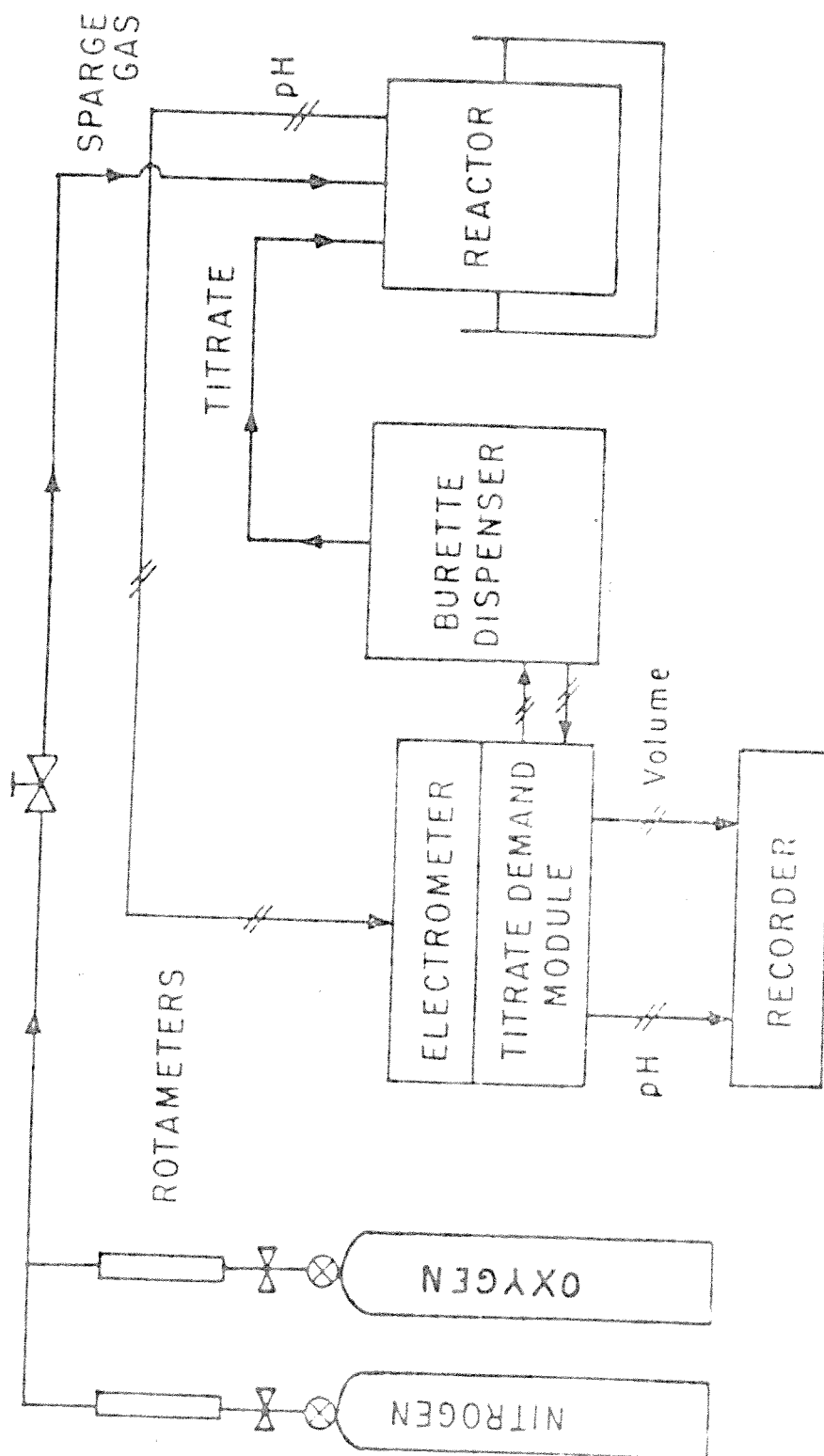


Figure 3.1 : Experimental Apparatus

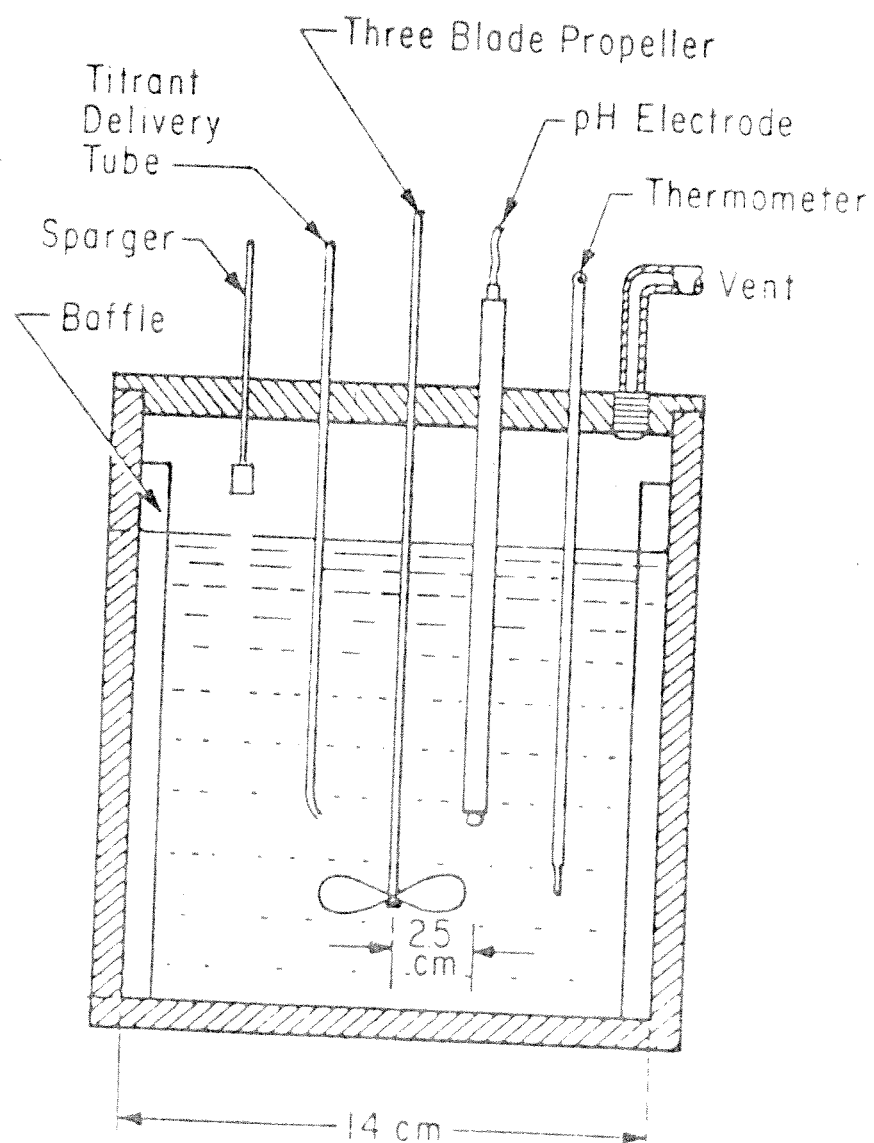


Figure 3.2 : Detailed Components of Reactor

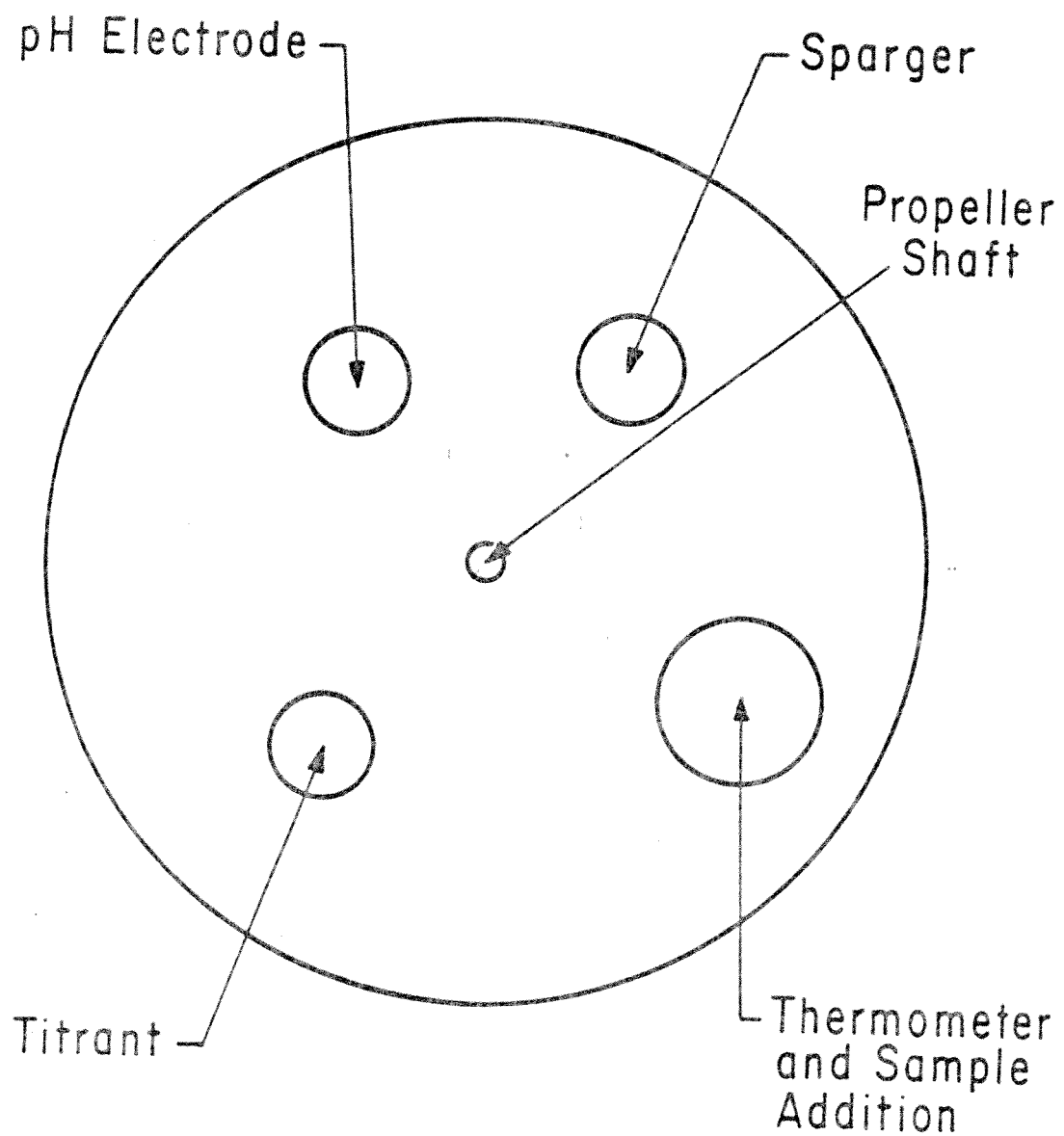


Figure 3.3 : Top View of Reactor Showing Orientations
of Each Component

by a needle valve. The flow system is presented in detail in Appendix C. The flow rate of the gas mixture was maintained at 250 ml/min (at 1 atm and 70°F) for all experimental runs. The low flow rate was desired to avoid a significant amount of SO₂ stripping.

The temperature of the reactor was kept constant at 50°C (except for two runs performed at 25 and 70°C) within 2°C by a water bath with a mercury on/off thermoregulator. The heat was supplied by an electric heating coil submerged in the bath. The temperature was measured by a thermometer. The gas mixture was pre-saturated with water at the experimental temperature to eliminate evaporation of water in the reactor.

The pH of the solution was measured by a combination electrode calibrated with standardized pH 4 phthalate and pH 7 phosphate buffers. The sulfite titrant was added through a slanted glass delivery tube.

The Fisher Electrometer and Titrate Demand Module consisted of a pH controller with proportional or on/off functions. A 10 ml digital burette was used for sulfite addition with a 10 mv recorder output and a two-pen linear recorder for pH and cumulative volume versus time.

Procedure

The plexiglass reactor was first filled with one liter of 0.3M sodium sulfate solution and placed in the water bath at the experimental temperature. Then, the solution was sparged below the liquid

surface by saturated N_2 for about 30 minutes in order to strip dissolved oxygen out of the solution. The relatively high sulfate concentration was chosen so that the small amount of sulfate ions produced during the experiment would not make a significant difference in its concentration. During this time the pH electrode was calibrated and a sodium sulfite solution placed in the automatic burette/dispenser. The concentration of the sulfite solution was 0.2 to 0.8 M depending on the expected sulfite demand. After these operations were completed the desired sodium bisulfite and catalyst amounts were added to the reactor, and the pH adjusted by adding either H_2SO_4 or NaOH. Finally, the gas sparger was removed from the solution and placed over the surface, and the desired O_2/N_2 mixture was allowed to flow at a rate of about 250 ml/min over the solution surface. The automatic burette/dispenser was started as soon as the gas mixture entered the reactor. Cumulative titrant volume and pH were recorded versus time on a two pen linear chart recorder.

All of the concentrations of the different solution components were either constant or insignificantly changed. Therefore, after the initial run was completed, the catalyst concentration was increased and a second data point was obtained. In the same manner several data points (6 to 8) were obtained during one experimental run. For the rate measurement at each catalyst concentration a titrant volume of 1 to 3 ml was added to the reactor solution. Thus, the liquid volume was increased by 0.1 to 0.3% for each measurement. These small volume

changes were neglected.

The catalysts (Mn and Fe) were added as $\text{MnSO}_4 \cdot \text{H}_2\text{O}$ and $\text{FeSO}_4 \cdot 7\text{H}_2\text{O}$. The inhibitor ($\text{S}_2\text{O}_3^{2-}$) was added as $\text{Na}_2\text{S}_2\text{O}_3 \cdot 5\text{H}_2\text{O}$.

Data Analysis

The oxygen absorption rate data was obtained directly from the rate of titrant (sulfite) addition to the reactor. The cumulative titrant volume added to the reactor was read off the recorder output within 0.02 ml. The time required for this addition was also obtained from the recorder output within 0.02 min. The titrant volume added to the reactor for each measurement was 1 to 3 ml, and the time was 5 to 30 minutes. After it was confirmed that the pH was constant (± 0.01 pH units) throughout the experiment, the O_2 absorption rate was obtained in moles/sec-cm² by:

$$\bar{R} = 1/2 \frac{V_t C_t}{t A} \times 10^{-3} \quad (3.4)$$

where V_t is the titrant volume added, ml; C_t is the titrant concentration, M; t is the experimental time, sec; and A is the reactor surface area, 154 cm².

Since the O_2/N_2 relative proportion was measured on a dry basis and the total pressure in the reactor was 1 atm, the oxygen partial pressure of the saturated gas mixture was calculated in atm by the relation:

$$P_{\text{O}_2} = X_{\text{O}_2} (1 - P_{\text{H}_2\text{O}}) \quad (3.5)$$

where X_{O_2} is the O_2 fraction in the O_2/N_2 gas mixture on a dry basis; and P_{H_2O} is the water vapor pressure at the experimental temperature, atm.

The oxygen concentration at the interphase was estimated by Henry's law:

$$[O_2]^* = P_{O_2} / H \quad (3.6)$$

where H is Henry's constant for oxygen in water, atm/M.

The mass transfer coefficients at 25 and 50°C were estimated by extrapolating the data obtained at 0.088 and 0.878 atm, respectively, to zero catalyst concentrations. The mass transfer coefficient at 70°C was obtained by making a measurement of the O_2 absorption rate at 70°C into a solution containing no catalyst. The k_L^* values, given in Table 4.1, were obtained by the relation:

$$k_L^* = \bar{R} / P_{O_2} \quad (3.7)$$

where \bar{R} is the oxygen absorption rate.

CHAPTER IV

RESULTS AND DISCUSSION

Three sets of data on oxygen absorption were obtained in 0.3 M Na_2SO_4 solutions with 0.01 M total sulfite at 470 rpm. In the first set effects of O_2 partial pressure, manganese concentration, and temperature were investigated. In the second set synergistic catalytic effects of dissolved Fe and Mn were examined. In the final set inhibiting effects of thiosulfate in the presence of Fe and Mn were studied. Additional data on the effects of pH, dissolved sulfite, and ionic strength are presented in Appendix B.

Manganese

Experimental runs with Mn were performed at constant oxygen pressure with Mn varying from 10^{-4} to 0.1 M. Runs were made at pH 5 with O_2 partial pressures from 0.018 to 0.878 atm. All runs were made at 50°C except for single runs at 25 and 70°C. The detailed experimental data are presented in tabular form in Appendix A, Table A.1.

A regression analysis on the data obtained at 50°C yielded the following model in the form of Equation 2.7:

$$\bar{R} = k_L^o [\text{O}_2]^* \left(1 + \frac{D_o k_1 [\text{Mn}]}{(k_L^o)^2 (1 + k_2 [\text{O}_2]^*)} \right)^{1/2} \quad (4.1)$$

where at 50°C, $k_1 = 3.80 \times 10^3$ l/sec-mole, and $k_2 = 8.28 \times 10^3$ l/mole. The experimental constants are shown in Table 4.1.

TABLE 4.1: Experimental Constants

Parameter	Symbol	Temperature (°C)	Value	Reference
Physical Absorption Coefficient	k_L°	25 50 70	4.61×10^{-3} cm/sec 7.07×10^{-3} cm/sec 1.14×10^{-2} cm/sec	Chapter 3
Oxygen Diffusivity	D_o	25 50 70	2.10×10^{-5} cm ² /sec 3.71×10^{-5} cm ² /sec 5.34×10^{-5} cm ² /sec	Sherwood (1975) * *
Henry's Law Constant	H	25 50 70	792 atm-l/mole 1072 atm-l/mole 1222 atm-l/mole	Sherwood (1925)

* Estimated by:

$$D_o = D_o^\circ \left(\frac{T}{T^\circ} \right)^{\frac{M_{H_2O}}{R}} \left(\frac{M_{H_2O}^\circ}{M_{H_2O}} \right)$$

The enhancement factor, E is:

$$E = \frac{k_L}{k_L^o} = \left(1 + \frac{D_o k_1 [Mn]}{(k_L^o)^2 (1 + k_2 [O_2]^*)} \right)^{1/2} \quad (4.2)$$

A complete comparison of the experimental data to the values predicted by the model is presented in Figure 4.1. Overall, the model predicts fairly accurate values; the greater deviations occur at low oxygen partial pressures (≤ 0.026 atm), and at high oxygen partial pressure (0.878 atm). The scatter at low E-1 is representative of random experimental error.

Note that the data used in developing the model were at constant sulfite concentration, pH, and ionic strength. Therefore, the model is a function of manganese concentration, oxygen partial pressure, and temperature only. The kinetic constant k_1 includes the effects of the other variables. Some data obtained as a function of sulfite concentration, pH, and ionic strength are presented and discussed in Appendix B. No major effect of these other variables was observed.

The general kinetic factor, γ defined in Equation 2.6 may now be redefined for the particular case in hand.

$$\gamma = \left(\frac{D_o k_1 [Mn] [O_2]^*}{(k_L^o)^2 (1 + k_2 [O_2]^*)} \right)^{1/2} \quad (4.3)$$

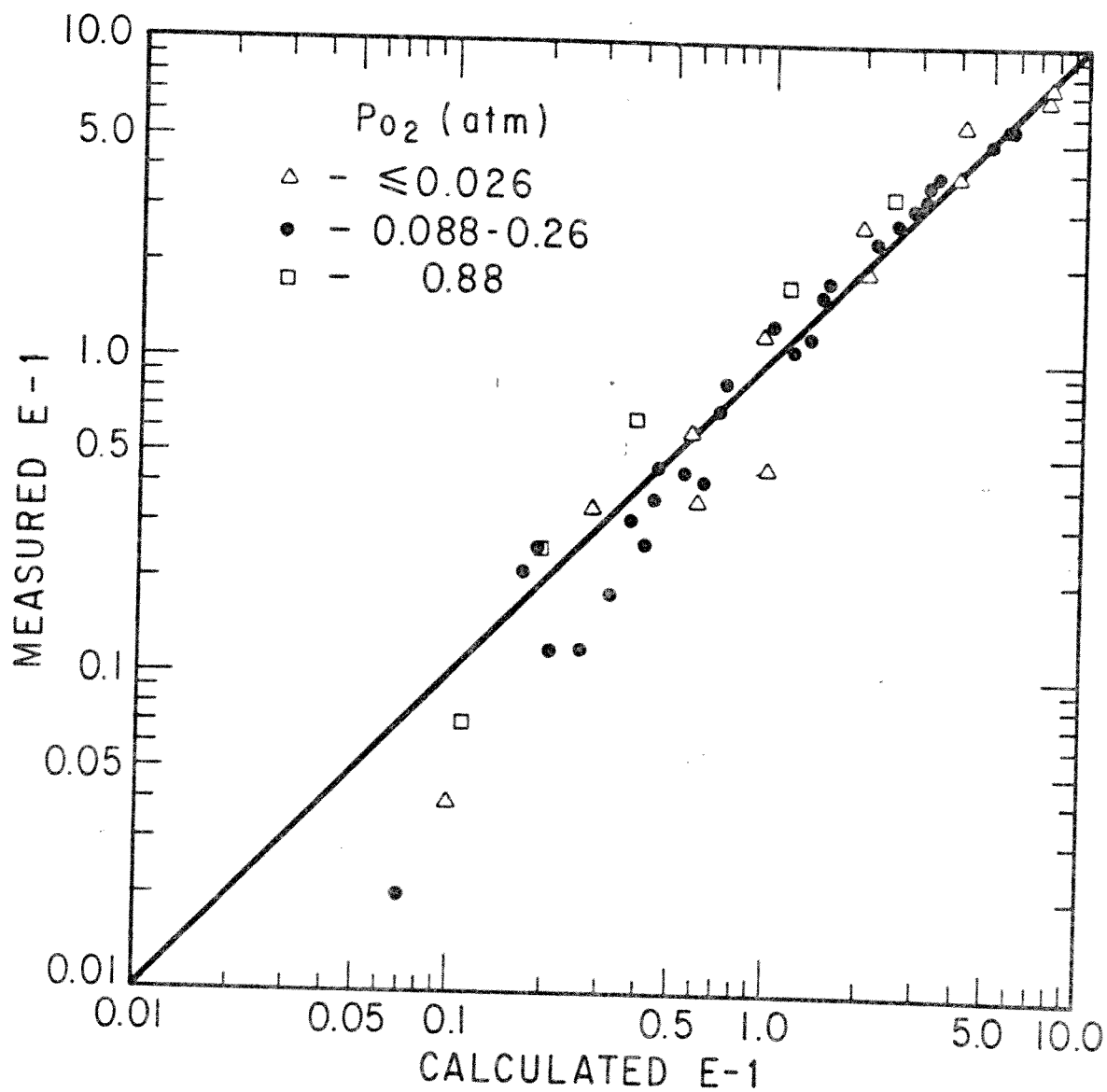


Figure 4.1: Comparison of calculated and measured values of the enhancement factor; pH 5, 50°C, 0.01 M sulfite, Mn from 10^{-4} to 0.10 M

At the lowest experimental O_2 partial pressure (0.018 atm) the γ values are 0.82 and 15.7 for Mn concentrations of 2.7 and 100 mM, respectively. At the highest O_2 pressure (0.878 atm) the γ values are 0.31 and 6.0, respectively. Therefore, the error introduced by the assumption used in solving Equation 2.1 is up to 6% at low manganese concentrations; the error becomes negligible as the manganese concentration is increased.

Effects of Manganese Concentration.-

The predicted and measured effects of Mn are illustrated for three O_2 partial pressures by Figure 4.2. At low Mn concentrations ($< 10^{-3}$ M) the absorption rate is dominated by physical absorption; hence, the slopes of the curves approach zero. As the Mn concentration is increased, the kinetic effect becomes the dominating factor and the slope of the curves increases until it reaches a value of 0.5. Therefore, the kinetics of the oxidation reaction are first order in manganese.

Effects of Oxygen Partial Pressure.-

Figure 4.3 illustrates the calculated and predicted mass transfer coefficient as a function of O_2 partial pressure. At 6.3 mM Mn the O_2 absorption rate is close to being limited by physical absorption; hence, the mass transfer coefficient has a weak dependence in oxygen. At 30 mM Mn, the kinetic effect becomes the dominating factor and the mass transfer coefficient is a strong function of O_2 partial pressure. As can be seen in Equation 4.3, the term containing

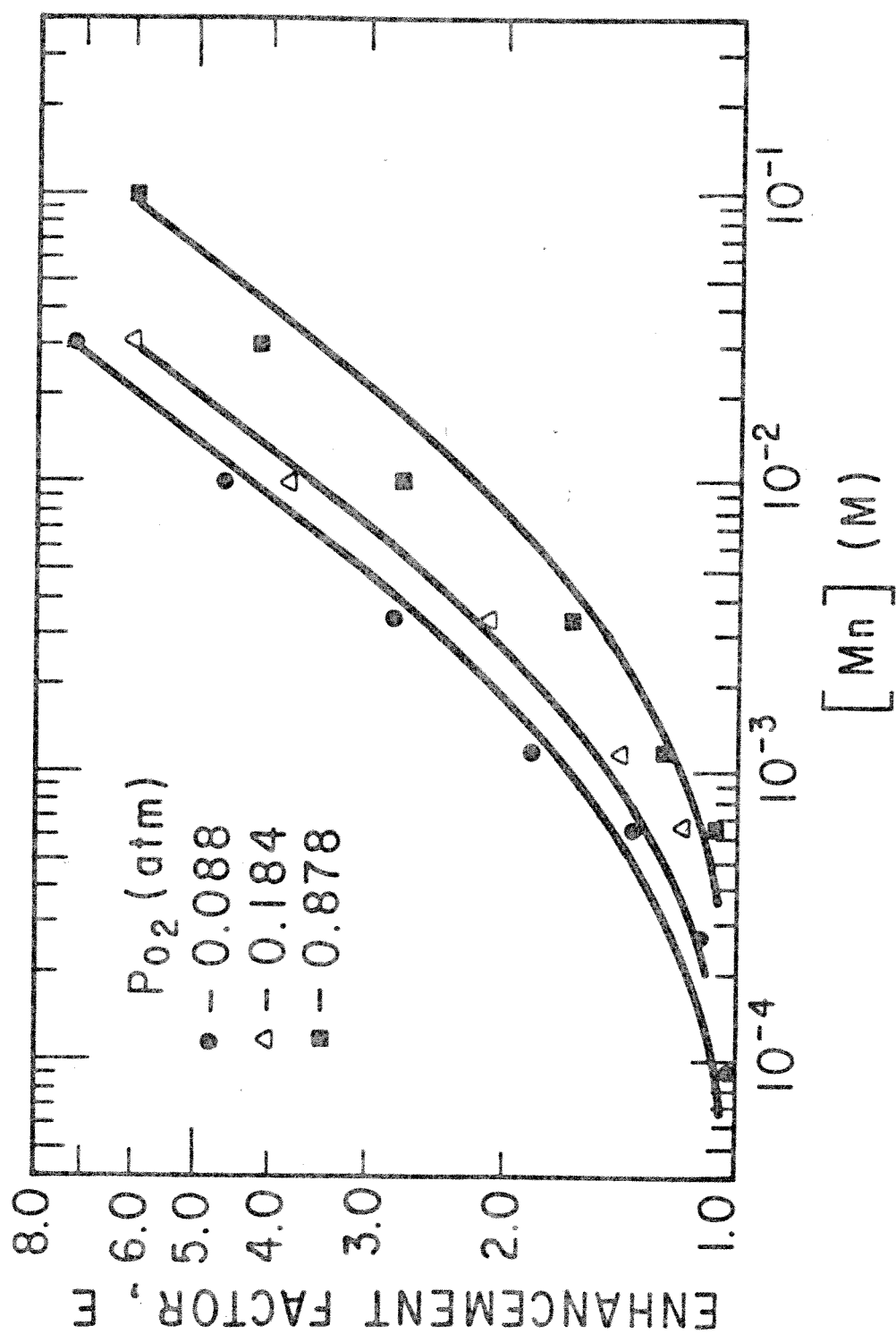


Figure 4.2: Enhancement factor as a function of manganese concentration; pH 5, 50°C, 0.01 M sulfite

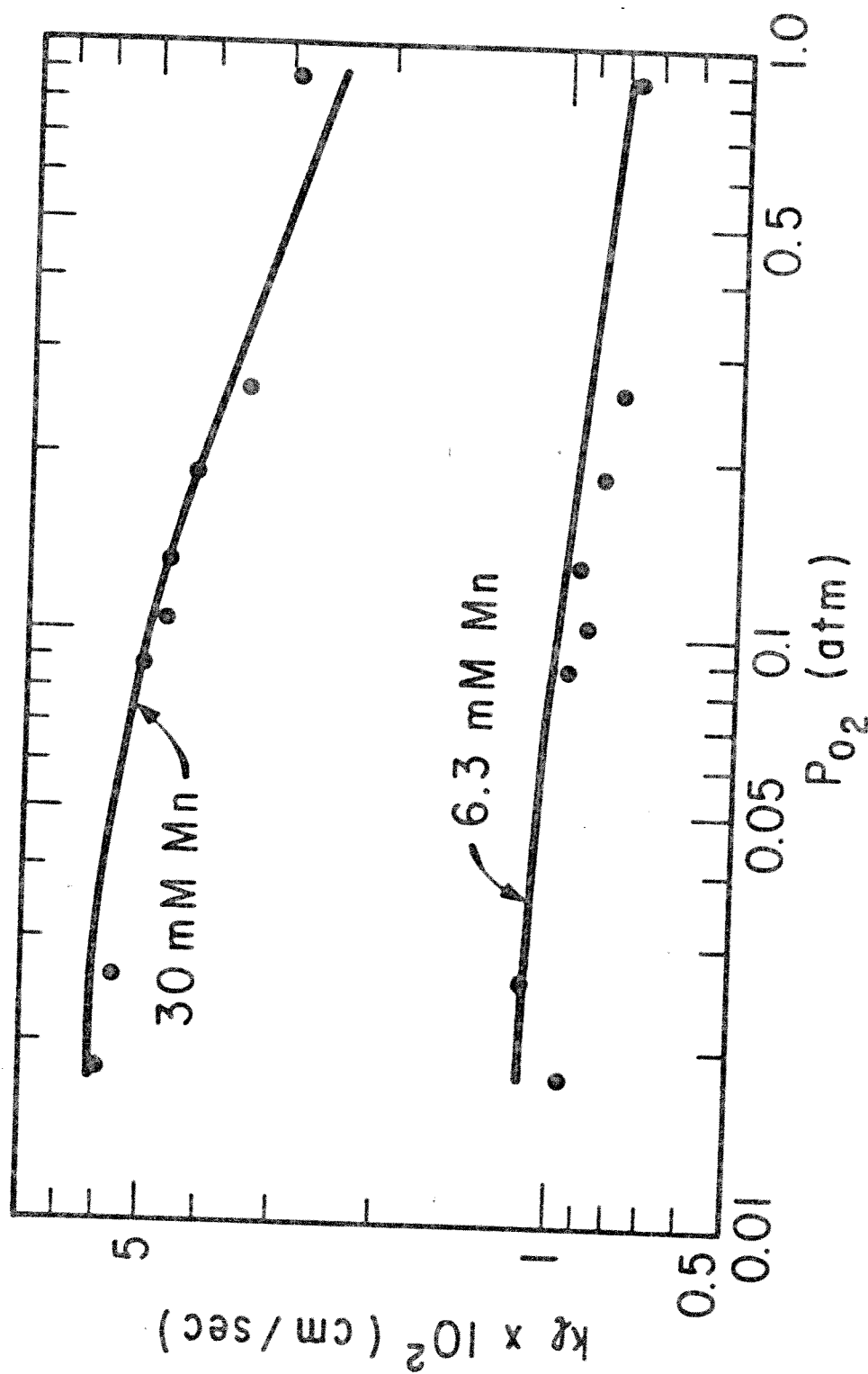


Figure 4.3: Mass Transfer Coefficient as a function of O_2 partial pressure and manganese concentration; pH 5, 50°C, and 0.01 M sulfite

the O_2 concentration effect in the overall kinetic factor is negligible at low oxygen partial pressures; hence, the mass transfer coefficient is independent of O_2 partial pressure in this region. As the O_2 pressure is increased, the O_2 concentration becomes significant and the mass transfer coefficient drops at an increasing rate. The slope of the curve drops until it reaches a value of -0.5.

The kinetic rate expression for sulfite oxidation derived from the above model (Equation 4.1) is:

$$r = \frac{k_1 [Mn] [O_2]}{1 + k_2 [O_2]} \quad (4.4)$$

where the rate, r is in moles/l-sec.

The rate is first order in manganese. It is first order in oxygen at low oxygen concentrations and zero oxygen at high oxygen concentrations. The same phenomenon of a drop in oxygen order as the O_2 concentration is increased was also observed by other researchers (Linek and Mayhoferova, 1970; Alper, 1973; Nyvlt and Kastanek, 1975; Onda et al, 1971). In their work using cobalt as catalyst under similar heterogeneous conditions they also found the catalyst to be first order; however, the oxygen order drop was from second to first.

Effects of Temperature.-

Since the oxygen absorption model contains two kinetic rate constants, two experimental runs were performed at two significantly different temperatures (25 and 70°C). The value Q , defined below,

which was a constant in each run was adjusted for the best statistical fit to the experimental data.

$$Q = \frac{D_o k_1 [O_2]^*}{1 + k_2 [O_2]^*} \quad (4.5)$$

The Q values were 6.85×10^{-10} and 1.06×10^{-10} at 70°C and 25°C , respectively. Substitution of Arrhenius expressions for the rate constant in Equation 4.5 at 25 and 70°C , and use of k_1 and k_2 values at 50°C gives a system of 4 equations. The solution of the equations yields the activation energies: $E_{a_1} = 18.1$ Kcal/mole, and $E_{a_2} = 23.4$ Kcal/mole. Figure 4.4 shows the predicted and measured mass transfer coefficients for runs at 25, 50, 70°C . Even though k_L differs at 50 and 70°C , the combined effects of temperature on rate constants, diffusivities, and oxygen solubility gives O_2 absorption rates which are nearly independent of temperature at 50 to 70°C .

Manganese and Iron

Experimental runs were performed with constant Fe and varying Mn, and with constant Mn and varying Fe. The experiments were performed at pH 4 and 50°C . Preliminary experiments gave no effect of FeSO_4 at pH 5, probably because of a low solubility of Fe. The detailed experimental data are presented in tabular form in Appendix A, Table A.2.

It is generally accepted that iron is a poor catalyst for sulfite oxidation compared to manganese (Bassett and Parker, 1951;

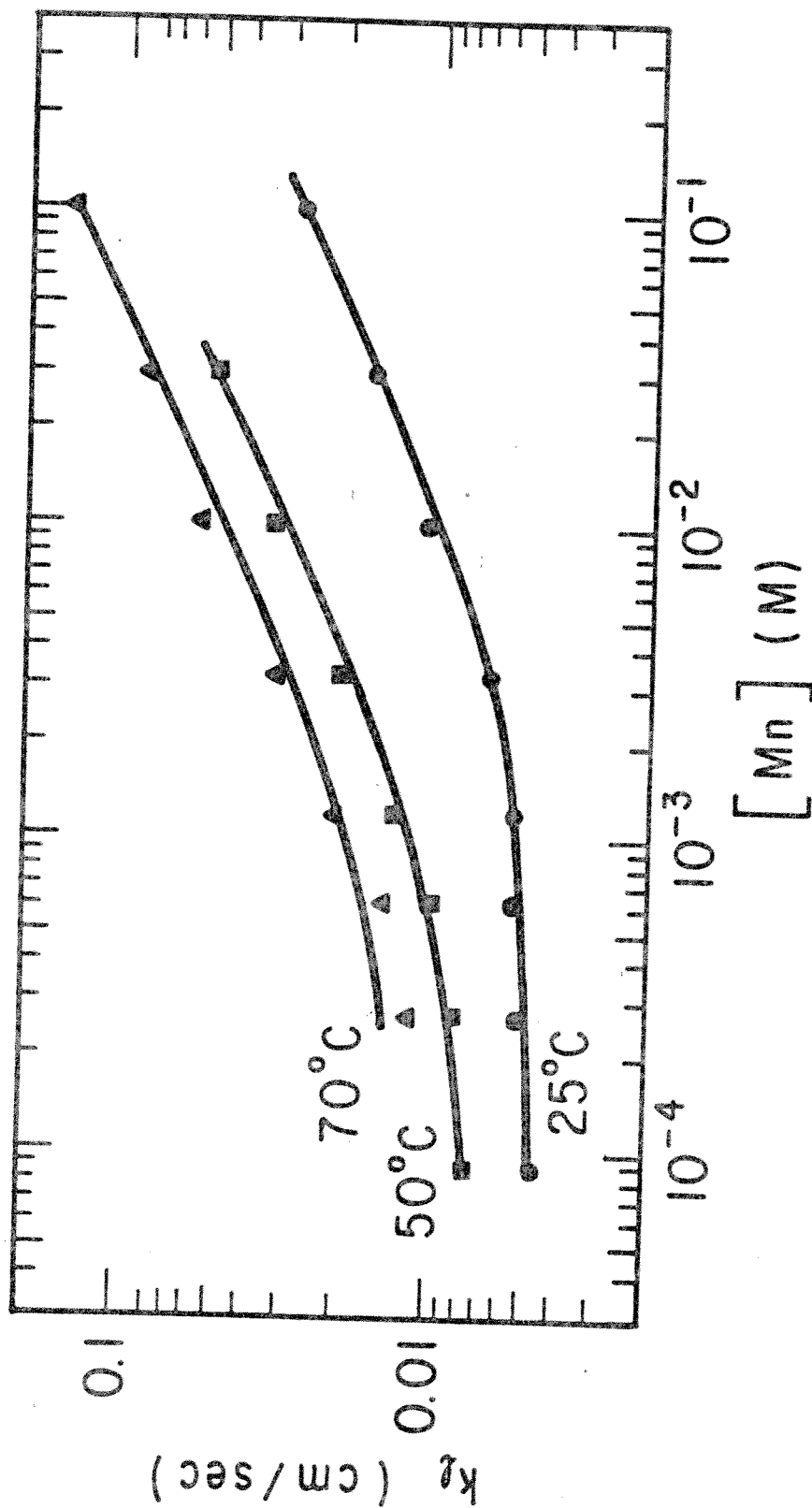


Figure 4.4: Mass Transfer Coefficient as a function of manganese concentration and temperature; pH 5, 0.088 atm O_2 , and 0.01 M sulfite

Johnstone and Coughanowr, 1958). However, using iron and manganese together Hudson (1980) found iron to have some significant effect. In his words: "It is noted that although the order of the reaction with respect to iron is zero, the results obtained with and without iron are different. Therefore, iron does influence the rate of reaction, but the rate does not depend on the amount of iron for $\text{Fe} > 1 \text{ ppm.}$ "

The results of this work for the effects of iron in the presence of manganese are illustrated in Figure 4.5. These experiments were done at different O_2 partial pressures with 0.01 M MnSO_4 . It was found that the iron order in the reaction rate is about 0.3. Even though the order of iron is relatively low, at 0.088 atm O_2 and 0.01 M Mn the mass transfer coefficient was found to be 0.035 and 0.055 cm/sec for 0.0 and 10^{-5} M Fe , respectively. Therefore, the presence of iron significantly accelerates the reaction.

The results for the effect of Mn in the presence of Fe are presented in Figure 4.6. The order of manganese with no iron present at pH 4 is about 1; the same result was found for pH 5. However, the presence of iron even in amounts as small as 0.3 mM greatly enhances the rate. No simple kinetic expression could model the discontinuity as O_2 absorption goes from control by physical absorption to control by reaction enhanced mass transfer. Instead, it is proposed that in the presence of iron at a "threshold" manganese concentration (1 to 2 mM) the manganese complexes in water change to a

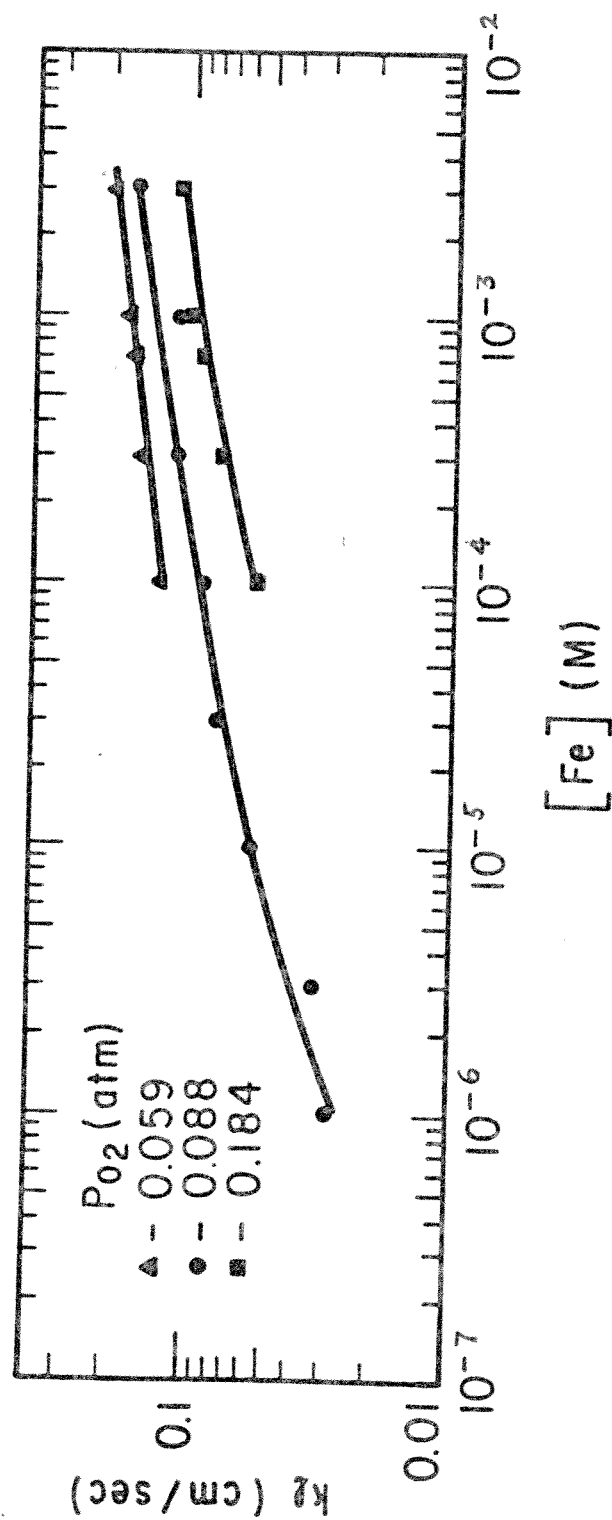


Figure 4.5: Mass Transfer coefficient as a function of iron concentration and O_2 partial pressure; pH 4, 50°C, 0.01 M sulfite, and 0.01 M $MnSO_4$

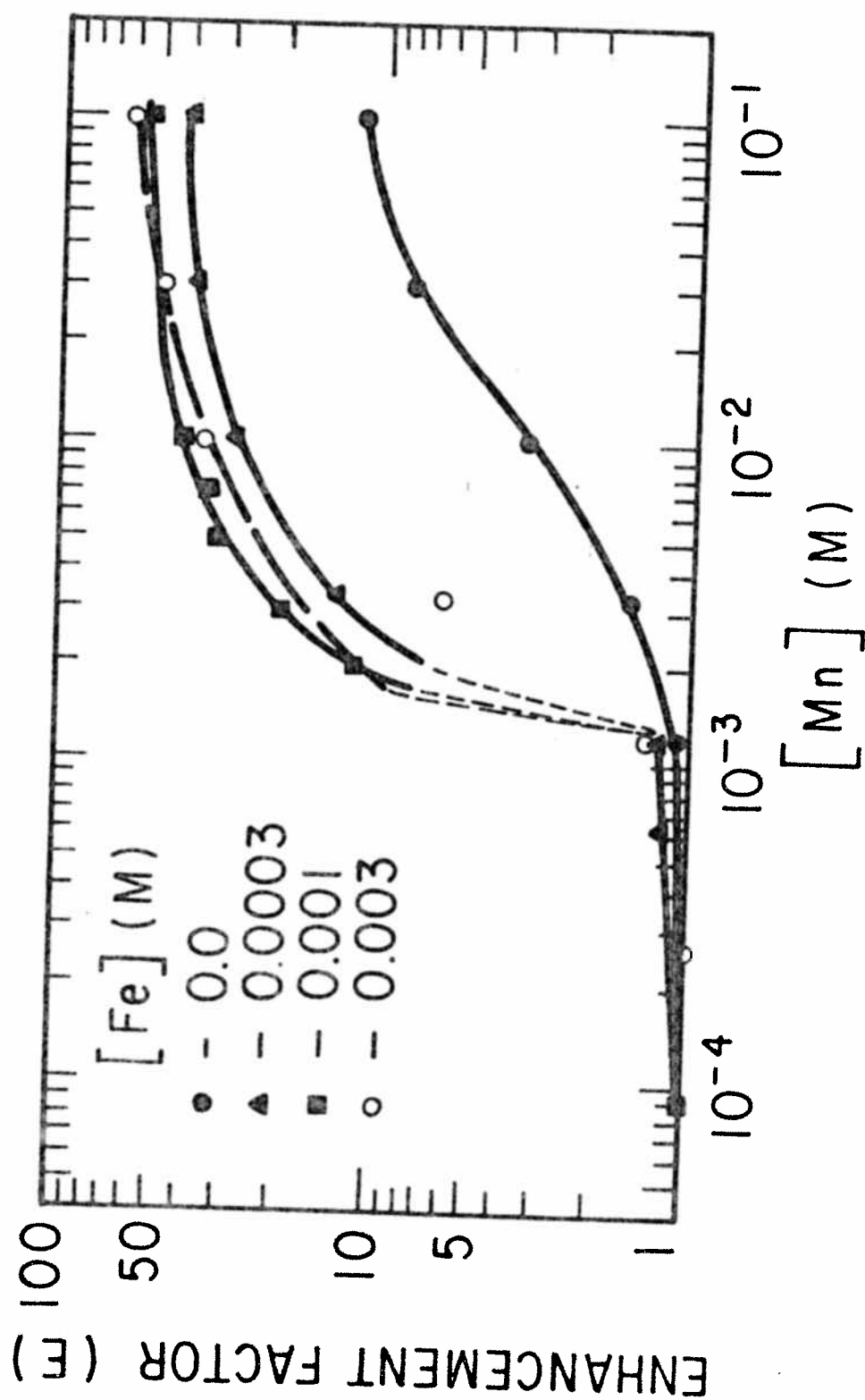


Figure 4.6: Enhancement factor as a function of Mn and Fe; pH 4, 50°C, 0.01 M sulfite, and 0.088 atm O_2

more active form. This does not necessarily mean that the Mn order is increased, but that the manganese catalytic activity is increased to yield greater reaction rates. That is, the kinetic rate constant is significantly increased by the change in the form of the manganese.

Linek and Vacek (1981) in their review article on sulfite oxidation catalyzed by cobalt and copper point out that the role of the catalyst has not yet been satisfactorily elucidated. There is no general agreement on the catalytic role of manganese either. Bassett and Parker (1951) contend that the active complex is $\text{Mn}(\text{SO}_3)_2^{-2}$. Brimblecombe and Spedding (1974b), in order to explain the zero order sulfite concentration dependence observed by some researchers, suggest that manganese is first oxidized to form MnOOH which would be the limiting reaction. No information was found on the possible catalytically active manganese-iron sulfite complexes.

Having Fe and Mn in solution can easily give enhancement factors of 20 to 100. Most limestone slurry scrubbers yield 10 to 20% oxidation of absorbed SO_2 when oxidation is limited by physical absorption. Therefore, it should be feasible to operate with a combination of Fe and Mn to obtain 100% oxidation in the scrubber. Operation at low pH would be required to keep the iron in solution, which may result in corrosion problems and may limit SO_2 absorption. A source of Fe and Mn may also be required if the desired amounts are not present in flyash or in limestone. The high concentrations of dissolved Fe and Mn may result in solid waste disposal problems.

Thiosulfate

In order to observe the effect of thiosulfate two experimental runs were performed at different conditions: 1) pH 4 and 3 mM Fe, and 2) pH 5 and 0.0 M Fe. Both runs were done at 50°C, 0.01 M MnSO_4 , and 0.088 atm O_2 with variable thiosulfate concentration. The detailed experimental data is presented in tabular form in Appendix A, Table A.3.

As illustrated by Figure 4.7, thiosulfate is a powerful inhibitor of the sulfite oxidation reaction. At a thiosulfate concentration of 1.0 mM the absorption rate was reduced by a factor of about 20; which corresponds to a reduction in the reactor velocity by a factor of about 400. At this point the absorption rate for the experimental run at pH 5 was below the physical absorption rate. Thus, the reaction rate was negligibly small and any further addition of thiosulfate would result in accumulation of O_2 in the bulk solution. The same observation is true at 2.0 mM thiosulfate for the experimental run at pH 4 and 3 mM Fe.

Hudson (1979), Radian (1977), and Rochelle et al (1982) have also observed that thiosulfate is a powerful inhibitor of sulfite oxidation.

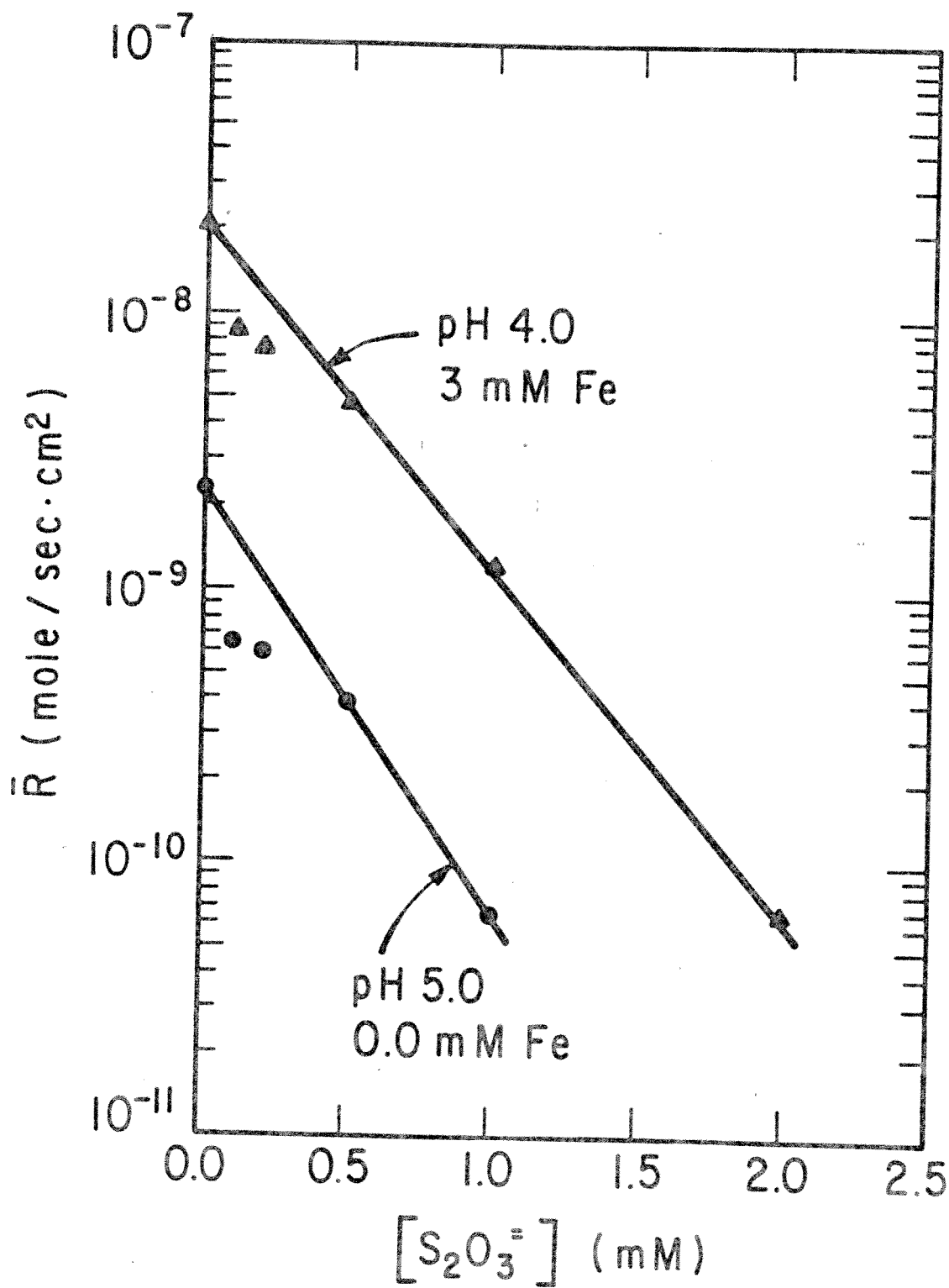


Figure 4.7: Inhibiting effect of thiosulfate; 50°C, 0.01 M sulfite, and 0.01 M MnSO₄

CHAPTER V

CONCLUSIONS AND RECOMMENDATIONS

Conclusions

1. Under heterogeneous conditions, with 0.01 M total sulfite, 0.3 M Na_2SO_4 , and pH 5.0, the rate of sulfite oxidation catalyzed by Manganese is given by:

$$r = \frac{k_1 [\text{Mn}] [\text{O}_2]}{1 + k_2 [\text{O}_2]}$$

where,

$$k_1 = 6.73 \times 10^{15} \exp(-18,100/RT)$$

$$k_2 = 5.65 \times 10^{19} \exp(-23,400/RT)$$

The rate is first order in O_2 at low O_2 partial pressures, and zero order at high O_2 pressures.

2. In order to observe a significant enhancement in the O_2 absorption rate at pH 5, a manganese concentration of 1 to 2 mM is required. A manganese concentration of 5 mM gives an enhancement of 2 to 5.

3. The presence of iron greatly enhances the oxygen absorption rate at Mn concentrations greater than 1 mM. At iron concentrations of 0.3 to 3 mM and pH 4, there is a threshold manganese concentration of 1 to 2 mM above which there is a discontinuous enhancement of 20 to 100 from physical absorption. In the presence of Fe, 5 mM Mn gives an enhancement of 20 to 50.

4. Thiosulfate is a powerful inhibitor of the sulfite oxidation reaction. A 1 mM thiosulfate concentration reduces the reaction velocity by a factor of about 400.

Recommendations

1. There is a need for fundamental research to quantify the role of the catalyst; that is, to determine which complexes are catalytically active and under which conditions they occur. Also, further research is needed to determine the Mn/Fe interactions in sulfite solutions.

2. Further work should be done to quantify simultaneous absorption of SO_2 and O_2 with catalysis by Mn/Fe. These results could be directly applicable as an innovation in throwaway slurry scrubbing.

APPENDIX A
EXPERIMENTAL DATA

TABLE A.1: Experimental Data - Mn Catalyzed Oxidation;

pH 5, 470 rpm, 0.01 M NaHSO_3 , and 0.3 M Na_2SO_4

RUN	T (°C)	[Mn] (M)	P_{O_2} (atm)	\bar{R}_{O_2} (mole/sec-cm ² x 10 ¹⁰)	E	k_L (cm/sec x 10 ³)
1	50	0.00009	0.018	1.24	1.04	7.35
		0.00063		1.62	1.36	9.62
		0.0012		1.73	1.45	10.3
		0.0033		3.52	2.95	20.9
		0.010		8.06	6.75	47.7
		0.030		10.1	8.47	59.9
2	50	0.00027	0.026	2.27	1.34	9.47
		0.00063		2.71	1.59	11.2
		0.0012		3.73	2.19	15.5
		0.0033		6.33	3.72	26.3
		0.010		8.39	4.94	34.9
		0.030		13.5	7.94	56.1
3	50	0.00009	0.088	5.95	1.02	7.21
		0.00027		6.55	1.12	7.92
		0.00063		7.95	1.36	9.62
		0.0012		10.8	1.85	13.1
		0.0033		16.2	2.79	19.7
		0.010		26.7	4.59	32.5
		0.030		42.1	7.22	51.0
4	50	0.00027	0.105	8.66	1.25	8.84
		0.00063		8.71	1.26	8.91
		0.0012		11.6	1.68	11.9
		0.0033		18.3	2.64	18.7
		0.010		30.4	4.39	31.0
		0.030		45.9	6.62	46.8
5	50	0.00027	0.132	10.6	1.21	8.55
		0.00063		11.5	1.31	9.26
		0.0012		12.3	1.41	9.97
		0.0033		19.4	2.21	15.6
		0.010		35.5	4.06	28.7
		0.030		57.4	6.58	46.5

(continued)

TABLE A.1: (continued)

RUN	T (°C)	[Mn] (M)	P _{O₂} (atm)	\bar{R}_{O_2} (mole/sec-cm ² x 10 ¹⁰)	E	k _L (cm/sec x 10 ³)
6	50	0.00063	0.184	14.4	1.18	8.34
		0.0012		17.5	1.44	10.2
		0.0033		25.5	2.09	14.8
		0.010		46.3	3.79	26.8
		0.030		73.6	6.02	42.6
7	50	0.00027	0.262	17.3	1.00	7.07
		0.00063		19.3	1.12	7.92
		0.0012		25.3	1.46	10.3
		0.0033		39.8	2.30	16.3
		0.010		60.1	3.47	24.5
8	50	0.00063	0.878	62.1	1.07	7.56
		0.0012		72.4	1.25	8.84
		0.0033		95.6	1.65	11.7
		0.010		159.	2.75	19.4
		0.030		240.	4.14	29.3
9	25	0.00009	0.097	5.62	1.00	4.61
		0.00027		6.26	1.11	5.11
		0.00063		6.59	1.17	5.38
		0.0012		6.53	1.16	5.33
		0.0033		7.88	1.39	6.43
10	70	0.00063	0.069	7.94	1.24	14.1
		0.0012		11.6	1.80	20.5
		0.0033		18.1	2.82	32.1
		0.010		32.4	5.04	57.4
		0.030		47.7	7.41	84.5
		0.10		83.7	13.0	148.

TABLE A.2: Experimental Data - Mn/Fe Catalyzed Oxidation;

pH 4, 50°C, 470 rpm, 0.01 M NaHSO₃, 0.3 M Na₂SO₄

RUN	P _{O₂} (atm)	[Mn] (M)	[Fe] (M)	\bar{R}_{O_2} (mole/sec-cm ² x 10 ¹⁰)	E	k _L (cm/sec x 10 ³)
11	0.059	0.010	0.0001	71.8	18.5	130.
			0.0003	84.2	21.6	153.
			0.0007	91.8	23.6	167.
			0.0010	95.6	24.6	174.
			0.0030	110.	28.3	200.
12	0.088	0.010	1.x 10 ⁻⁶	23.2	4.00	28.3
			3.x 10 ⁻⁶	27.8	4.79	33.9
			1.x 10 ⁻⁵	47.0	8.10	57.2
			3.x 10 ⁻⁵	63.2	10.9	77.0
			0.0001	71.8	12.4	87.5
			0.0003	91.3	15.7	111.
			0.0010	90.2	15.6	110.
			0.0030	130.	22.4	158.
13	0.132	0.010	0.0001	67.0	7.69	54.4
			0.0003	100.	11.5	81.2
			0.0007	130.	14.9	106.
			0.0010	146.	16.8	119.
			0.0030	185.	21.2	150.
14	0.184	0.010	0.0001	93.4	7.72	54.4
			0.0003	132.	10.9	76.9
			0.0007	153.	12.6	89.1
			0.0010	170.	14.1	99.0
			0.0030	188.	15.5	110.
15	0.088	0.00009	0.0003	5.97	1.03	7.28
		0.00063		6.97	1.20	8.48
		0.0012		7.66	1.32	9.33
		0.0033		80.1	13.8	97.6
		0.010		167.	28.8	204.
		0.030		220.	37.9	268.
		0.10		224.	38.6	273.

(continued)

TABLE A.2: (continued)

RUN	P_{O_2} (atm)	$[Mn]$ (M)	$[Fe]$ (M)	\bar{R}_{O_2} (mole/sec-cm ² $\times 10^{10}$)	E	k_L (cm/sec $\times 10^3$)
16	0.088	0.00009	0.0010	5.92	1.02	7.21
		0.0020		68.5	11.8	83.4
		0.0030		118.	20.4	144.
		0.0050		187.	32.3	228.
		0.0070		215.	37.1	262.
		0.010		247.	42.5	300.
		0.030		356.	61.3	433.
		0.10		332.	57.2	404.
17	0.088	0.00027	0.0030	5.80	1.00	7.07
		0.0012		7.71	1.33	9.40
		0.0033		35.1	6.06	42.8
		0.010		206.	35.6	252.
		0.030		280.	48.3	341.
		0.10		300.	51.7	366.
18	0.088	0.00009	0.0	5.86	1.01	7.14
		0.00027		6.03	1.04	7.35
		0.00063		5.97	1.03	7.28
		0.0012		6.32	1.09	7.71
		0.0033		8.93	1.54	10.9
		0.010		22.4	3.87	27.4
		0.030		46.0	7.93	56.1
		0.10		67.3	11.6	82.0

TABLE A.3: Experimental Data - Thiosulfate Inhibited Oxidation;

50°C, 0.088 atm P_{O_2} , 470 rpm, 0.01 M $NaHSO_3$,
 0.3 M Na_2SO_4 .

RUN	pH	$[Mn]$	$[Fe]$	$[S_2O_3^{-2}]$	\bar{R}_{O_2}
		(M)	(M)	(M)	(mole/sec-cm ² x 10 ¹⁰)
19	5.0	0.010	0.0	0.0	21.6
				0.0001	6.21
				0.0002	5.99
				0.0005	3.89
				0.0010	0.756
				0.0020	*
20	4.0	0.010	0.003	0.0	120.
				0.0001	83.7
				0.0002	76.1
				0.0005	49.3
				0.0010	12.6
				0.0020	0.648
				0.0050	*

* The minimum oxygen absorption rate that is possible to measure in the experimental apparatus used in this work is about $1. \times 10^{-11}$ mole/sec-cm²; this rates were significantly less than the minimum values.

APPENDIX B

SULFITE, pH, IONIC STRENGTH, AND ELECTROLYTE DATA

Sulfite Data

Experimental runs were made at constant manganese concentration with total sulfite varying from 0.0005 to 0.10 M. The runs were made at 50°C and pH 5.0 with 0.088 and 0.262 atm O_2 , and with 0.0027, 0.027, and 0.0033 M Mn. Sulfite was added to the reactor as $NaHSO_3$ and the procedure was the same as that for the catalyst scans described in Chapter 3. After each $NaHSO_3$ addition the pH was readjusted by adding NaOH.

The experimental data are shown in tabular form in Table B.1. Some preliminary calculations using approximate equations (Hikita and Asai, 1964) suggest that the rise in the absorption rate with sulfite at low sulfite concentrations is not a sulfite concentration effect; but that the surface reaction is being limited by the sulfite diffusion from the bulk. At a sulfite concentration of 0.005 M the reaction is no longer limited by sulfite diffusion. At the lower Mn concentrations (0.0027 and 0.0033 M) the absorption rate decreases with sulfite (> 0.005 M) suggesting that sulfite inhibits the reaction at high concentrations. The same effect was also observed by Laurent et al (1974), Onda et al (1971), Astarita et al (1964), and Wesselingh and van't Hoog (1970). At high catalyst concentrations (0.027 M) the absorption rates were approximately constant at sulfite concentrations greater than 0.005 M suggesting that the reaction is zero order with respect to sulfite.

TABLE B.1: Experimental Data - Dependence on Sulfite Concentration;
 pH 5, 50°C, 470 rpm, and 0.3 M Na₂SO₄

RUN	P _{O₂} (atm)	[Mn] (M)	[Total Sulfite] (M)	\bar{R}_{O_2} (mole/sec-cm ² x 10 ¹⁰)
21	0.088	0.027	0.0005	31.5
			0.0010	69.6
			0.0030	109.
			0.010	135.
			0.030	148.
22	0.262	0.027	0.0005	100.
			0.0010	137.
			0.0030	213.
			0.010	218.
			0.030	216.
23	0.088	0.0033	0.10	205.
			0.0005	56.8
			0.0010	69.8
			0.0020	76.7
			0.0050	78.4
24	0.262	0.0033	0.010	71.5
			0.020	60.5
			0.050	50.8
			0.10	43.4
			0.0005	86.0
			0.0010	105.
			0.0020	114.
			0.0050	115.
			0.010	105.
			0.020	90.5
			0.050	80.4
			0.10	59.2

(continued)

TABLE B.1: (continued)

RUN	P_{O_2} (atm)	$[Mn]$ (M)	$[Total\ Sulfite]$ (M)	\bar{R}_{O_2} (mole/sec-cm ² x 10 ¹⁰)
25	0.088	0.0027	0.0010	46.9
			0.0030	53.6
			0.010	51.2
			0.030	42.8
			0.10	32.4
26	0.262	0.0027	0.0005	68.0
			0.0010	76.9
			0.0030	85.8
			0.010	81.6
			0.030	68.3
			0.10	59.2

pH Data

The experimental pH runs consisted of O_2 absorption rate measurements in the pH range of 4 to 7. The experiments were performed at 0.088 and 0.262 atm P_{O_2} , and 0.001 and 0.05 M total sulfite. All the data were collected at 50°C and 0.01 M Mn. Each experimental run was started at pH 4 and the pH was adjusted for every measurement by adding concentrated NaOH. The procedure was similar to that described in Chapter 3.

The experimental data are shown in tabular form in Table B.2. At the lower sulfite concentration (0.001 M) the O_2 absorption rate increased with pH until reaching a maximum at pH 5; there after it decreased with increasing pH. At the higher sulfite concentration (0.05 M) the absorption rate varied in the same manner with pH, but it reached a maximum at a pH of 5.5 and 6.0 for O_2 partial pressures of 0.088 and 0.262 atm, respectively. A similar effect of pH was observed by Brimblecombe and Spedding (1974b) who for the oxidation of SO_2 in "pure" water in the range of pH 4 to 8.5 found the rate to be a maximum at pH 6.0.

Ionic Strength Data

Since all but a negligible ionic strength is supplied by Na_2SO_4 in the experimental data presented in this thesis, the ionic strength effect was observed by measurements at Na_2SO_4 concentrations in the range of 0.03 to 1.0 M. The experimental run was made at 50°C, pH 5, 0.088 atm P_{O_2} , 0.01 M $NaHSO_3$, and 0.0033 M $MnSO_4$.

TABLE B.2: Experimental Data - pH Dependence; 50°C, 470 rpm,
0.01 M MnSO_4 , 0.3 M Na_2SO_4 .

RUN	P_{O_2} (atm)	[Total Sulfite] (M)	pH	\bar{R}_{O_2} (mole/sec-cm ² x 10 ¹⁰)
27	0.088	0.001	4.0	38.7
			4.5	90.3
			5.0	98.1
			5.5	91.2
			6.0	51.8
			6.5	40.2
			7.0	34.8
28	0.088	0.050	4.5	133.
			5.0	198.
			5.5	233.
			6.0	81.6
			6.5	76.7
			7.0	52.9
29	0.262	0.001	4.0	132.
			4.5	115.
			5.0	307.
			5.5	170.
			6.0	201.
			6.5	198.
			7.0	184.
30	0.262	0.050	4.0	124.
			4.5	92.7
			5.0	137.
			5.5	242.
			6.0	367.
			6.5	216.
			7.0	209.

The experimental data is presented in Table B.3. The O_2 absorption rate increased with increasing sodium sulfate until reaching a maximum at a concentration of 0.2 M, there after it decreased with increasing Na_2SO_4 concentration.

Electrolyte Data

In order to observe the effect of the environment on sulfite oxidation under heterogeneous conditions some data was collected in $MgSO_4$ and $MgCl_2$ solutions. The experimental runs consisted of measurements of O_2 absorption rates while varying the manganese concentration from 0.09 mM to 0.1 M in 0.3 M solutions of either $MgSO_4$ or $MgCl_2$. The experiments were performed at 50°C, pH 5, 0.01 M $NaHSO_3$, and 0.132 and 0.262 atm O_2 .

The experimental data is shown in tabular form in Table B.4. First order kinetics in manganese were observed. The O_2 absorption rates were slightly greater in $MgSO_4$ and $MgCl_2$ solutions than in Na_2SO_4 solutions. At high O_2 partial pressure (0.262 atm) the absorption rates were faster in $MgSO_4$ solutions, while at a lower O_2 pressure (0.132 atm) the absorption rates were faster in $MgCl_2$ solutions.

TABLE B.3: Experimental Data - Dependence on Na_2SO_4 concentration;
 50°C , pH 5, 470 rpm, 0.088 atm P_{O_2} , 0.01 M NaHSO_3 , and
 0.0033 M MnSO_4 .

RUN	$[\text{Na}_2\text{SO}_4]$	\bar{R}_{O_2} (mole/sec-cm ² x 10 ¹⁰)
	(M)	
31	0.030	55.9
	0.070	62.2
	0.10	68.0
	0.20	71.5
	0.50	62.2
	1.0	55.7

TABLE B.4: Experimental Data - Dependence on Electrolyte; 50°C, pH 5,
470 rpm, and 0.01 M NaHSO₃.

RUN	P _{O₂} (atm)	Electrolyte (0.3 M)	[Mn] (M)	\bar{R}_{O_2} (mole/sec-cm ² x 10 ¹⁰)
32	0.132	MgSO ₄	0.00009	50.5
			0.00027	62.0
			0.00063	65.2
			0.0012	76.9
			0.0033	108.
			0.010	168.
			0.030	231.
			0.10	300.
33	0.262	MgSO ₄	0.00009	121.
			0.00027	165.
			0.00063	187.
			0.0012	220.
			0.0033	298.
			0.010	445.
			0.030	594.
			0.10	823.
34	0.132	MgCl ₂	0.00009	49.7
			0.00027	63.3
			0.00063	74.1
			0.0012	77.5
			0.0033	103.
			0.010	197.
			0.030	378.
			0.10	400.
35	0.262	MgCl ₂	0.00009	139.
			0.00027	136.
			0.00063	130.
			0.0012	130.
			0.0033	156.
			0.010	257.
			0.030	462.
			0.10	631.

APPENDIX C
GAS FLOW SYSTEM

Gas Flow System

Nitrogen and Oxygen gas were supplied by two cylinders with the pressure regulators set at 80 and 20 psi, respectively. In addition to a control valve each line had a needle valve for precise flow rate control. The individual flow rates were measured by two low flowrate rotameters. The rotameters were calibrated using a wet test meter; the calibration curves for O_2 and N_2 are shown in Figures C.1 and C.2, respectively. After the flow rate measurements were made, the gases flowed into a single line. Then, the gas mixture was saturated with water at the experimental temperature. The saturation process consisted of sparging the gas mixture in water about 7 cm below the surface using a fritted glass dispersion tube. Finally, the gas mixture was allowed to flow over the reactor solution surface.

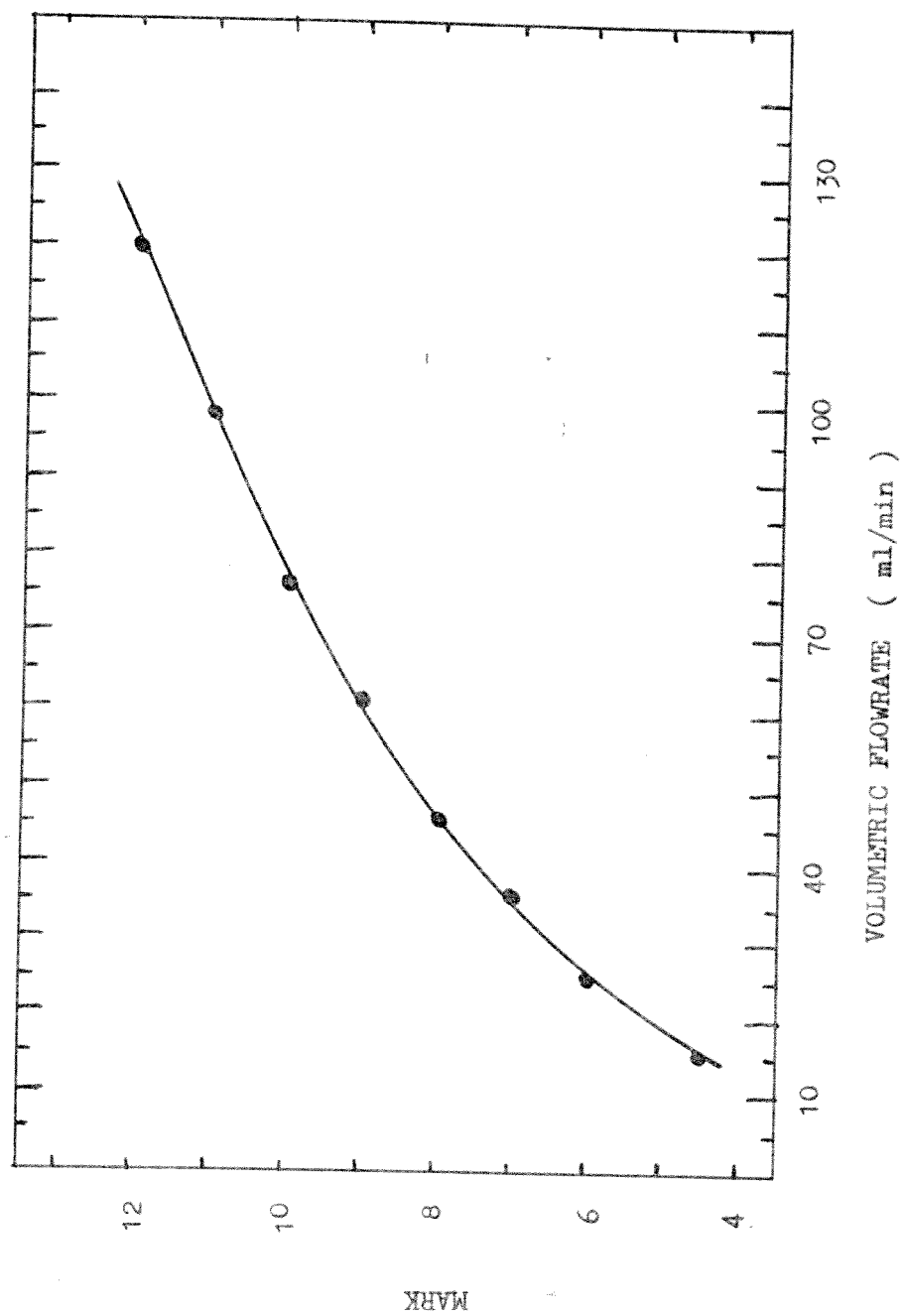


Figure C.1 : Oxygen Rotameter Calibration Curve

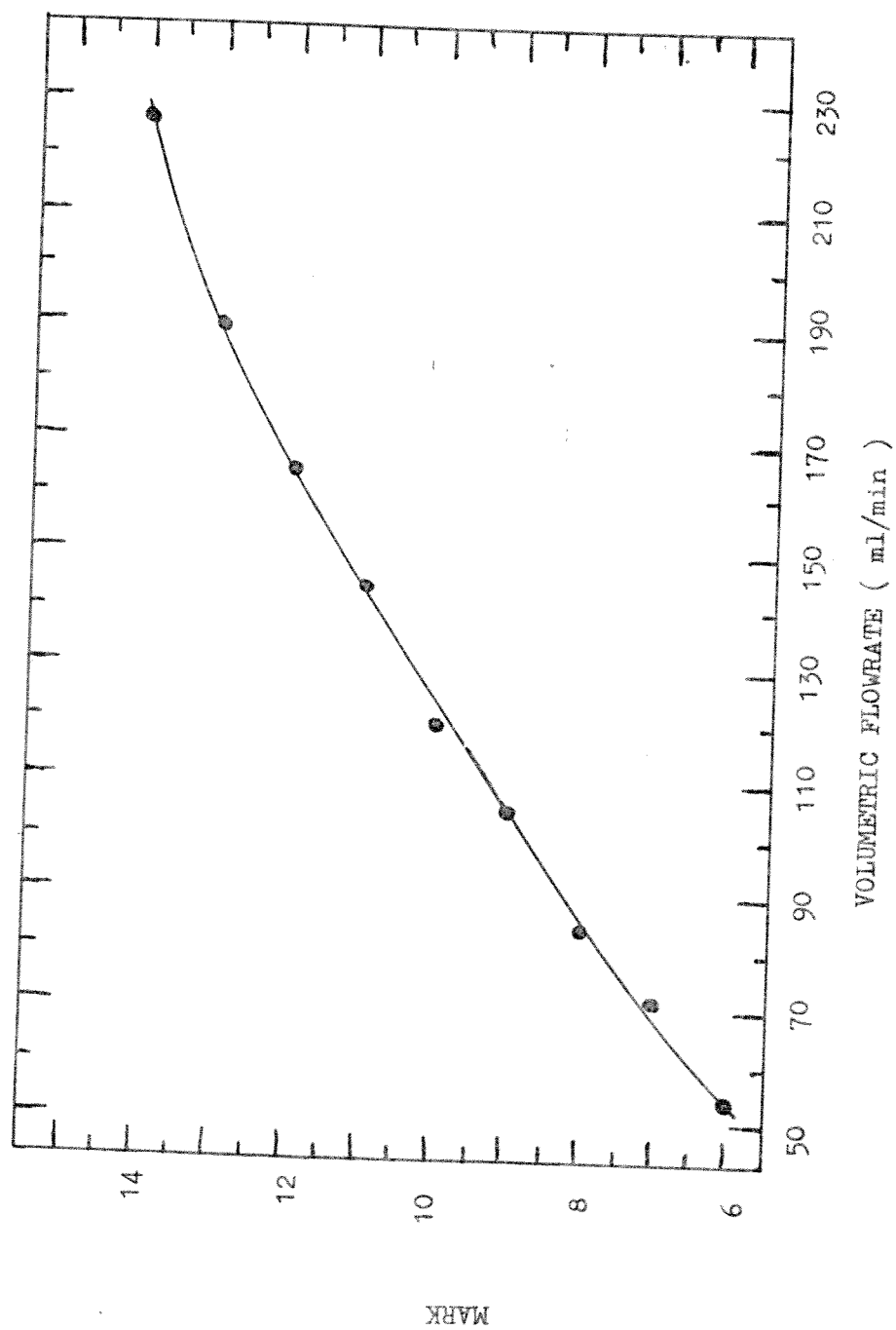


Figure C.2 : Nitrogen Rotameter Calibration Curve

APPENDIX D
MASS BALANCE AT THE INTERFACE

Mass Balance at the Interface

A model was developed in order to estimate the concentrations at the gas-liquid interface. The model consisted of the following equations:

$$2 \bar{R} = k_{\text{HSO}_3^-} \Delta [\text{HSO}_3^-] + k_{\text{SO}_3^{2-}} \Delta [\text{SO}_3^{2-}] \quad (\text{D.1})$$

$$K_{\text{HSO}_3^-} = [\text{H}^+]_s [\text{SO}_3^{2-}]_s / [\text{HSO}_3^-]_s \quad (\text{D.2})$$

$$f k_{\text{H}^+} \Delta [\text{H}^+] = - k_{\text{HSO}_3^-} \Delta [\text{HSO}_3^-] \quad (\text{D.3})$$

where

\bar{R} = absorption rate,

K_i = equilibrium constant for i ,

k_i = liquid mass transfer coefficient for i ,

Δ = bulk - interface, and

f = factor included to account for the acidity transport due to HSO_4^- .

The factor, f was estimated by:

$$f = \left(\frac{D_{\text{HSO}_4^-}}{D_{\text{H}^+}} \right)^{1/2} [\text{SO}_4^{2-}] / K_{\text{HSO}_4^-} + 1.0 \quad (\text{D.4})$$

The bulk concentrations were calculated using Equation D.2 and the equations,

$$[\text{total sulfite}] = [\text{SO}_3^{2-}] + [\text{HSO}_3^-] \quad (\text{D.5})$$

$$[\text{H}^+] = 10^{-\text{pH}} \quad (\text{D.6})$$

The liquid mass transfer coefficients were calculated by:

$$k_i = \left(\frac{D_i}{D_o} \right)^{1/2} k_L^o \quad (D.7)$$

where the O_2 liquid mass transfer coefficient, $k_L^o = 7.07 \times 10^{-3}$ at $50^\circ C$.

The values of the constants used in the mass balance are presented in Table D.1.

The results for all the manganese catalyzed runs at $50^\circ C$ and pH 5 are tabulated in Table D.2. As expected, there was no significant total sulfite concentration difference between the bulk and the interface; but there was a significant drop in pH at the interface.

TABLE D.1: Constants For the Mass Balance at the Interface at 50°C.

<u>Parameter</u>	<u>value</u>
D_O	$3.72 \times 10^{-5} \text{ cm}^2/\text{sec}$
$D_{\text{SO}_3^{2-}}$	$1.24 \times 10^{-5} \text{ cm}^2/\text{sec}$
D_{H^+}	$1.65 \times 10^{-4} \text{ cm}^2/\text{sec}$
$D_{\text{HSO}_3^-}$	$2.35 \times 10^{-5} \text{ cm}^2/\text{sec}$
$D_{\text{HSO}_4^-}$	$2.12 \times 10^{-5} \text{ cm}^2/\text{sec}$
$k_{\text{SO}_3^{2-}}$	$4.08 \times 10^{-3} \text{ cm} / \text{sec}$
$k_{\text{HSO}_3^-}$	$5.62 \times 10^{-3} \text{ cm}/\text{sec}$
k_{H^+}	$1.49 \times 10^{-2} \text{ cm}/\text{sec}$
$\text{pK}_{\text{HSO}_3^-}$	6.8
$\text{pK}_{\text{HSO}_4^-}$	1.4
f	3.70

TABLE D.2: Comparison of Bulk and Interface pH and Total Sulfite
Concentration at 50°C

RUN	Mn (M)	Total Sulfite (M)		pH	
		Bulk	Interface	Bulk	Interface
1	0.00009	0.01000	0.00995	5.0	4.91
	0.00063		0.00993		4.88
	0.0012		0.00993		4.87
	0.0033		0.00986		4.75
	0.010		0.00969		4.50
	0.030		0.00961		4.42
2	0.00027	0.01000	0.00991	5.0	4.84
	0.00063		0.00989		4.81
	0.0012		0.00985		4.74
	0.0033		0.00975		4.59
	0.010		0.00967		4.49
	0.030		0.00949		4.30
3	0.00009	0.01000	0.00976	5.0	4.61
	0.00027		0.00974		4.58
	0.00063		0.00969		4.51
	0.0012		0.00958		4.39
	0.0033		0.00939		4.23
	0.010		0.00902		4.02
4	0.00027	0.01000	0.00966	5.0	4.48
	0.00063		0.00966		4.48
	0.0012		0.00956		4.37
	0.0033		0.00932		4.18
	0.010		0.00889		3.96
	0.030		0.00834		3.78
5	0.00027	0.01000	0.00959	5.0	4.40
	0.00063		0.00956		4.37
	0.0012		0.00953		4.34
	0.0033		0.00928		4.16
	0.010		0.00871		3.89
	0.030		0.00793		3.68

(continued)

TABLE D.2: (continued)

RUN	Mn (M)	Total Sulfite (M)		pH	pH
		Bulk	Interface		
6	0.00063	0.01000	0.00946	5.0	4.28
	0.0012		0.00934		4.20
	0.0033		0.00906		4.04
	0.010		0.00832		3.78
	0.030		0.00736		3.58
7	0.00027	0.01000	0.00935	5.0	4.20
	0.00063		0.00927		4.15
	0.0012		0.00907		4.04
	0.0033		0.00855		3.84
	0.010		0.00784		3.66
	0.030		0.00696		3.51

APPENDIX E

NOTATION

NOTATION

- A = Reactor surface area, 154 cm^2
 γ = Kinetic factor defined by Equation 2.6
 C_t = Titrant concentration, M
 D_i = Diffusion coefficient of i in water, cm^2/sec
 D_o = Diffusion coefficient of O_2 in water, cm^2/sec
 D_s = Diffusion coefficient of sulfite in water, cm^2/sec
 E = O_2 absorption rate enhancement factor
 H = Henry's Law constant for O_2 in water, atm-l/mole
 $k_{1,2}$ = Kinetic rate constant
 k_i = Mass transfer coefficient of i in water, cm/sec
 k_L = O_2 physical mass transfer coefficient, cm/sec
 k_L = O_2 enhanced mass transfer coefficient, cm/sec
 K_i = Equilibrium constant for i
 $[O_2]^*$ = Equilibrium O_2 concentration in aqueous solution at a particular temperature and oxygen partial pressure, M
 P_{H_2O} = Water vapor pressure, atm
 P_{O_2} = Oxygen partial pressure, atm
 Q = Constant factor for each run defined by Equation 4.5
 r_o = Oxygen reaction rate, $\text{mole}/\text{sec-l}$
 r_s = Sulfite reaction rate, $\text{mole}/\text{sec-l}$
 R = Gas constant, $1.987 \text{ cal}/\text{mole}^\circ\text{K}$
 \bar{R} = Oxygen absorption rate, $\text{mole}/\text{sec-cm}^2$

t = Experimental time, sec

T = Experimental temperature, °K

V_t = Titrant volume, ml

x = Distance from the surface, cm

X_{O_2} = O_2 volumetric fraction of the O_2/N_2 gas mixture on a dry basis

REFERENCES CITED

- Alper, E., "Kinetics of Oxidation of Sodium Sulfite solution," Trans. Inst. Chem. Eng., 51, 159 (1973).
- Astarita, G., G. Marrucci, and L. Coletti, "Catalytic Oxidation of Na_2SO_3 - Measure the Interfacial Area," Chim. e L'Ind., 46, 1021 (1964).
- Backstrom, H. L. J., "The Chain Mechanism in the Auto-Oxidation of Sodium Sulfite Solutions," Z. Phys. Chem., B25, 99 (1934).
- Barron, C. H. and H. A. O'Hern, "Reaction Kinetics of Sodium Sulfite Oxidation by the Rapid Mixing Method," Chem. Eng. Sci., 21, 397 (1966).
- Bassett, H. and W. G. Parker, "The Oxidation of Sulphurous Acid," J. Chem. Sci., 1540 (1951).
- Bengtsson, S. and I. Bjerle, "Catalytic Oxidation of Sulfite in Diluted Aqueous Solutions," Chem. Eng. Sci., 30, 1429 (1975).
- Braga, T. G. and E. Connick, "Mechanism of the Oxidation of Bisulfite Ion by Oxygen," Presented at Spring ACS 1981 Meeting.
- Brimblecombe, P. and D. J. Spedding, "The Reaction Order of the Metal Ion Catalyzed Oxidation of Sulfur Dioxide in Aqueous Solutions," Chemosphere, 3, 29 (1974a).
- Brimblecombe, P. and D. J. Spedding, "The Catalytic Oxidation of Micromolar Aqueous Sulphur Dioxide-I," Atmos. Environ., 8, 937 (1974b).

- Chen, T. I. and C. H. Barron, "Some Aspects of the Homogeneous Kinetics of Sulfite Oxidation," Ind. Eng. Chem. Fund., 11, 466 (1972).
- Chertkov, B. A., "Theory of Oxidation of Sulfite-Bisulfite Solutions," Zh. Priklab. Khim., 32, 2609 (1959).
- Coughanowr, D. R. and F. E. Krause, "The Reaction of SO_2 and O_2 in Aqueous Solutions of MnSO_4 ," Ind. Eng. Chem. Fund., 4(1), 61 (1965).
- Danckwerts, P. V., Gas-Liquid Reactions, McGraw-Hill Inc., USA (1970).
- Hayon, E., A. Treining, and J. Wolf, "Electronic Spectra, Photochemistry, and Autoxidation Mechanism of the Sulfite-Bisulfite-Pyrosulfite Systems," J. Amer. Chem. Soc., 94, 47 (1972).
- Hikita, H. and S. Asai, "Gas Absorption with (m,n)th Order irreversible Chemical Reaction," Int. Chem. Eng., 4(2), 332 (1964).
- Hudson, J. L., "Sulfur Dioxide Oxidation in Scrubber Systems," Monthly Progress Report, March 1979, EPA Grant Number R805227-02-0.
- Hudson, J. L., "Sulfur Dioxide Oxidation in Scrubber Systems," EPA-600/7-80-083, (1980).
- Johnstone, H. F. and D. R. Coughnowr, "Absorption of Sulfur Dioxide from Air," Ind. Eng. Chem. Fund., 50(8), 1169 (1958).
- Laurent, A., J. C. Charpentier, and C. Prost, "Total Heterogeneous Kinetics of the Catalytic Oxidation of Sodium Sulfite Solution by Gaseous Oxygen in the Presence of Cobalt Sulfate," J. Chim. Phys., 71, 613 (1974).

- Linek, V. and J. Mayrhoferova, "The Kinetics of Oxidation of Aqueous Sodium Sulfite Solutions," Chem. Eng. Sci., 25, 787 (1970).
- Linek, V. and V. Vacek, "Chemical Engineering Use of Catalyzed Sulfite Oxidation Kinetics for the Determination of Mass Transfer Characteristics of Gas-Liquid Contactors," Chem. Eng. Sci., 36, 1747 (1981).
- Mishra G. C. and R. D. Srivastava, "Kinetics of Heterogeneous Oxidation of Ammonium Sulfite," Chem. Eng. Sci., 31, 969 (1976).
- Nyvt, V. and F. Kastanek, "Gas-Liquid Reactors. VI. Interfacial Area in a Bubble Type Plate Reactor," Coll. Czech. Chem. Commun., 40, 1853 (1975).
- Onda, K., H. Takeuchi, and Y. Maeda, "The Absorption of Oxygen into Sodium Sulphite Solutions in Packed Column," Chem. Eng. Sci., 27, 449 (1972).
- Radian Corporation, "Characterization of Carbide Lime to Identify Sulfite Oxidation Inhibitors," EPA-600/7-78-176, Sept, 1978.
- Reith, T. and W. J. Beek, "The Oxidation of Aqueous Sodium Sulphite Solutions," Chem. Eng. Sci., 28, 1337 (1973).
- Rochelle, G. T. and C. J. King, "Alternatives for Stack Gas Desulfurization by Throwaway Scrubbing," Chem. Eng. Prog., 74(2), 65 (1978).
- Rochelle, G. T., W. T. Weems, R. J. Smith, and M. W. Hsiang, "Buffer Additives for Lime/Limestone Slurry Scrubbing," ACS Symp. Ser., In Press (1982).

Sawicki, J. E. and C. H. Barron, "Kinetics of Sulfite Oxidation in Heterogeneous Systems," Chem. Eng. J., 5, 153 (1973).

Sherwood, T. K., "Solubilities of SO_2 and NH_3 in water," Ind. Eng. Chem., 17, 745 (1925).

Sherwood, T. K., R. L. Pigford, and C. R. Wilke, Mass Transfer, McGraw-Hill Inc., New York (1975).

Wesselingh, J. A. and A. C. van't Hoog, "Oxidation of Aqueous Sulfite Solutions: Model Reaction for Measurements in Gas-Liquid Dispersions," Trans. Inst. Chem. Eng., 48, T69 (1970).

OXYGEN ABSORPTION ENHANCED BY SULFITE OXIDATION CATALYZED WITH
MANGANESE AND IRON

APPROVED:

To my parents, Rolando and Teresa

ACKNOWLEDGEMENTS

I would like to express my sincere appreciation for the attention and guidance of Dr. Gary T. Rochelle on this project. I am grateful to have had the opportunity to work with him. I would also like to thank Dr. James R. Fair for acting as my second reader, his comments and suggestions were sincerely appreciated.

Thanks are due to the supporters of Dr. G. T. Rochelle's work for their financial support of this project.

Finally, I would like to give my love to my family for their support and encouragement over the years.

Roberto E. Prada

December, 1981

VITA

Roberto Eduardo Prada was born in Cochabamba, Bolivia on August 3, 1958, the son of Teresa Prada and J. Rolando Prada. After completing his work at Saint Andrew's School, La Paz, Bolivia, in 1975, he entered The University of Texas at Austin in Austin, Texas. He received the degree of Bachelor of Science in May, 1980 with a major in Chemical Engineering. In September, 1980, he entered The Graduate School of The University of Texas in The Department of Chemical Engineering.

Permanent address: Casilla 2620

La Paz, Bolivia

This thesis was typed by the author.